Zoological Journal of the Linnean Society, 2024, **202**, zlae156
https://doi.org/10.1093/zoolinnean/zlae156
Advance access publication 16 December 2024
Original Article

Original Article

New specimens of *Saturnalia tupiniquim* (Dinosauria: Sauropodomorpha): insights into intraspecific variation, rostral anatomy, and skull size

Lísie V.S. Damke[1,2,*], Max C. Langer[3], Átila A.S. Da-Rosa[1,4], Rodrigo T. Müller[1,2]

[1]Programa de Pós-Graduação em Biodiversidade Animal, Universidade Federal de Santa Maria, Santa Maria, Brazil
[2]Centro de Apoio à Pesquisa Paleontológica da Quarta Colônia, Universidade Federal de Santa Maria, São João do Polêsine, Brazil
[3]Departamento de Biologia, FFCLRP, Universidade de São Paulo, Ribeirão Preto, Brazil
[4]Laboratório de Estratigrafia e Paleobiologia, Universidade Federal de Santa Maria, Santa Maria, Brazil

[*]Corresponding author. Programa de Pós-Graduação em Biodiversidade Animal, Universidade Federal de Santa Maria, Santa Maria, Brazil. E-mail: lisiesd@hotmail.com

ABSTRACT

Dinosaurs arose in the Late Triassic and diversified during the subsequent periods of the Mesozoic Era. The oldest unequivocal dinosaurs come from Carnian deposits of Brazil, Argentina, India, and Zimbabwe, with sauropodomorphs representing the bulk of this record. *Saturnalia tupiniquim* was described from Brazilian strata in 1999 as the first Carnian member of that group. Although several new species and specimens of coeval sauropodomorphs have been described in recent years, no new material has been formally assigned to that species. In this contribution, we describe an association of at least three partially preserved individuals of *S. tupiniquim* (UFSM 11660), which was excavated from the *S. tupiniquim* type-locality (Late Triassic of the Santa Maria Formation) and preserves cranial and postcranial elements, including the first rostrum known for the species. Assigned to *S. tupiniquim* according to several lines of evidence, the new specimen has a proportionally short rostrum, compared to that of coeval sauropodomorphs, providing evidence for a reduced skull in *S. tupiniquim*. In addition, we investigated the intraspecific variation in *S. tupiniquim*, highlighting the need to understand the morphological limits of such variations among the earliest dinosaurs, in order to properly explore their alpha diversity.

Keywords: systematics; Saurischia; Triassic; Carnian

INTRODUCTION

Dinosaurs are one of the most fascinating groups of land vertebrates, usually divided in two main lineages, Ornithischia and Saurischia, with the latter composed of Theropoda and Sauropodomorpha (Nesbitt 2011, Langer *et al.* 2017, Ezcurra *et al.* 2020, Novas *et al.* 2021, Norman *et al.* 2022, see Baron *et al.* 2017 for different interpretations). In the Brazilian Triassic, Sauropodomorpha is the most abundant dinosaurian clade (Novas *et al.* 2021, Langer *et al.* 2022), corresponding to small bipedal faunivorous animals (Sereno *et al.* 2013, Cabreira *et al.* 2016, Müller *et al.* 2018a) that substantially differ from their exaggeratedly large, quadrupedal, and herbivorous younger 'successors' (McPhee *et al.* 2018, Apaldetti *et al.* 2021).

Saturnalia tupiniquim was the first Triassic sauropodomorph discovered from Brazil (Langer *et al.* 1999) and, as the first unambiguously recognized Carnian member of the group worldwide, its type series played a key role in understanding the body plan of early sauropodomorphs. In the following years, numerous other sauropodomorphs were discovered from Carnian beds of Argentina, Brazil, and Zimbabwe (Martínez and Alcober 2009, Ezcurra 2010, Cabreira *et al.* 2011, 2016, Ezcurra 2010, Cabreira *et al.* 2011, 2016, Pretto *et al.* 2018, Griffin *et al.* 2022), allowing us to understand the first steps of their evolution, distribution, diversity, and biology (Bronzati *et al.* 2017, Müller *et al.* 2018b, Langer *et al.* 2022, Dunne *et al.* 2023). However, after the description of the holotype and paratypes of *S. tupiniquim*, no other material was formally referred to the species (but see Garcia *et al.* 2019b), hampering a better understanding of the intraspecific variation and anatomy of this taxon (Langer *et al.* 2022). In this contribution, we describe a new association of *S. tupiniquim* specimens, which provides new data on the rostral anatomy and intraspecific variation of this dinosaur.

Received 10 June 2024; revised 22 October 2024; accepted 6 November 2024

Institutional abbreviations

CAPPA/UFSM, Centro de Apoio à Pesquisa Paleontológica da Quarta Colônia da Universidade Federal de Santa Maria, Rio Grande do Sul, Brazil; LPRP/USP, Laboratório de Paleontologia de Ribeirão Preto, Universidade de São Paulo, Ribeirão Preto, Brazil; SMNS, Staatliches Museum für Naturkunde, Germany; PVSJ, Division of Vertebrate Paleontology of the Museo de Ciencias Naturales de la Universidade Nacional de San Juan, San Juan, Argentina; UFRGS-PV, Paleovertebrate Collection of the Laboratório de Paleovertebrados da Universidade Federal do Rio Grande do Sul, Porto Alegre, Brazil; UFSM, Coleção de Paleontologia do Laboratório de Estratigrafia e Paleobiologia, Universidade Federal de Santa Maria, Santa Maria, Brazil; ULBRA, Centro de Apoio à Pesquisa Paleontológica da Quarta Colônia, Universidade Federal de Santa Maria, São João do Polêsine, Rio Grande do Sul, Brazil (previously Museu de Ciências Naturais, Universidade Luterana do Brasil, Canoas, Brazil).

MATERIAL AND METHODS

Material

UFSM 11660 comprises an assemblage of at least three individuals, disarticulated to partially articulated, found in a small area of about 1 m^2 (Fig. 1) in the type-locality of *S. tupiniquim*. All elements have the typical morphology of early dinosaurs and there are no significant differences between overlapping bones, so that we interpret UFSM 11660 as a monotypic association. Although the minimal number of individuals is three, given the triplicated sacral remains, it is not unlikely that the association is composed of more individuals (see Systematic Palaeontology).

Phylogenetic analyses

In order to explore the phylogenetic position of UFSM 11660, it was scored as a whole in two different phylogenetic matrices. In both analyses we employed the original parameters, briefly recapped here. We first scored UFSM 11660 in the data matrix of Norman *et al.* (2022) in order to test the putative placement of UFSM 11660 among sauropodomorphs. We performed an heuristic search, with 1000 replicates of Wagner Trees (random seed = 0) + tree bisection reconnection (TBR) and 20 trees saved per replicate. The characters were ordered as in the original analysis and all characters received the same weight.

The second set of analyses was performed with UFSM 1160 scored in the data matrix of Langer *et al.* (2022), in order to explore the position of UFSM 11660 in an alpha taxonomic assessment of Carnian sauropodomorphs. As in the original study, we performed two analyses with this data matrix. First, all specimens of *S. tupiniquim* (*N* = 3), *Buriolestes schultzi* (*N* = 2), and *Eoraptor lunensis* (*N* = 3) were treated as separate operational taxonomic units (OTUs). In the subsequent analysis, the specimens were merged into single OTUs for each one of these three species. The three analyses were performed employing a heuristic search with 1000 replicates of Wagner trees holding 10 trees per replicate (random seed = 0). The scoring of UFSM 11660 and the modifications in the character matrix are listed in the Supporting information.

Morphological disparity

To test the position of UFSM 11660 in the early sauropodomorph morphospace, we performed a morphological disparity analysis, following the same parameters and data matrix employed by Langer *et al.* (2022). The R package Claddis 0.6.3 (Lloyd 2016) was used to calculate the distance matrix with the Maximum Observable Rescaled Distance (Lloyd 2016, Lehmann *et al.* 2019). An ordination matrix was generated with a Principal Coordinate Analysis (PCoA), employing the Lingoes correction for negative eigenvalues. Subsequently, we performed a PERMANOVA (Permutational Multivariate Analysis of Variance) with *adonis2* of vegan package (2.6-4) to test for a significant difference in the morphospace occupied by the referred materials of *S. tupiniquim*, *Bu. schultzi*, and *E. lunensis*.

Skull length estimate

To estimate the skull length, we employed a least squares regression using the maxillary length as a predictive variable to skull length. This was based on a dataset compiled for Triassic sauropodomorphs, as seen in Table 1.

SYSTEMATIC PALAEONTOLOGY

Dinosauria Owen, 1842 *sensu* Langer *et al.* 2020
Saurischia Seeley, 1888 *sensu* Gauthier *et al.* 2020
Sauropodomorpha Huene, 1932 *sensu* Fabbri *et al.* 2020
Saturnalia tupiniquim Langer *et al.* 1999

Holotype

MCP 3844-PV (Langer *et al.* 1999, Langer 2003, 2007b) comprising some skull remains, most presacral vertebrae, two primordial sacral vertebrae, several proximal caudal vertebrae, several cervical and trunk ribs, partial scapular girdle and forelimbs, most of the pelvic girdle and hindlimbs.

Paratypes

MCP 3845-PV (Langer *et al.* 1999, Langer 2003, 2007b, Bronzati *et al.* 2017, 2019a, b) is composed of a semi-articulated skeleton, comprising a partial skull with braincase, natural cast of mandibular ramus with teeth, most presacral vertebrae, two primordial sacral vertebrae plus a dorsosacral vertebra, several cervical and trunk ribs, right scapular girdle and forelimb, most of the pelvic girdle and hindlimbs. MCP 3846-PV (Langer *et al.* 1999, Bittencourt *et al.* 2012, Garcia *et al.* 2019b) is an incomplete skeleton, comprising some presacral and caudal vertebrae and parts of the pelvic girdle and hindlimbs.

Referred specimen UFSM 11660 (A–N)

An association of at least three individuals with different degrees of articulation. It comprises a partial skull with braincase, lower jaws, vertebrae from distinct portions of the column, ribs, chevrons, pelvic girdle, femora, tibiae, metatarsals, and phalanges. Because of its gracile morphology, the specimen was affectionately nicknamed as 'Gracinha', meaning graceful in Portuguese. The specific preserved elements are: UFSM 11660A, skull, right maxilla, braincase elements; UFSM 11660B, dorsal vertebrae; UFSM 11660C, sacrum articulated against the ilium, ischium, pubis; UFSM 11660D, partial sacrum; UFSM 11660E, damaged sacrum;

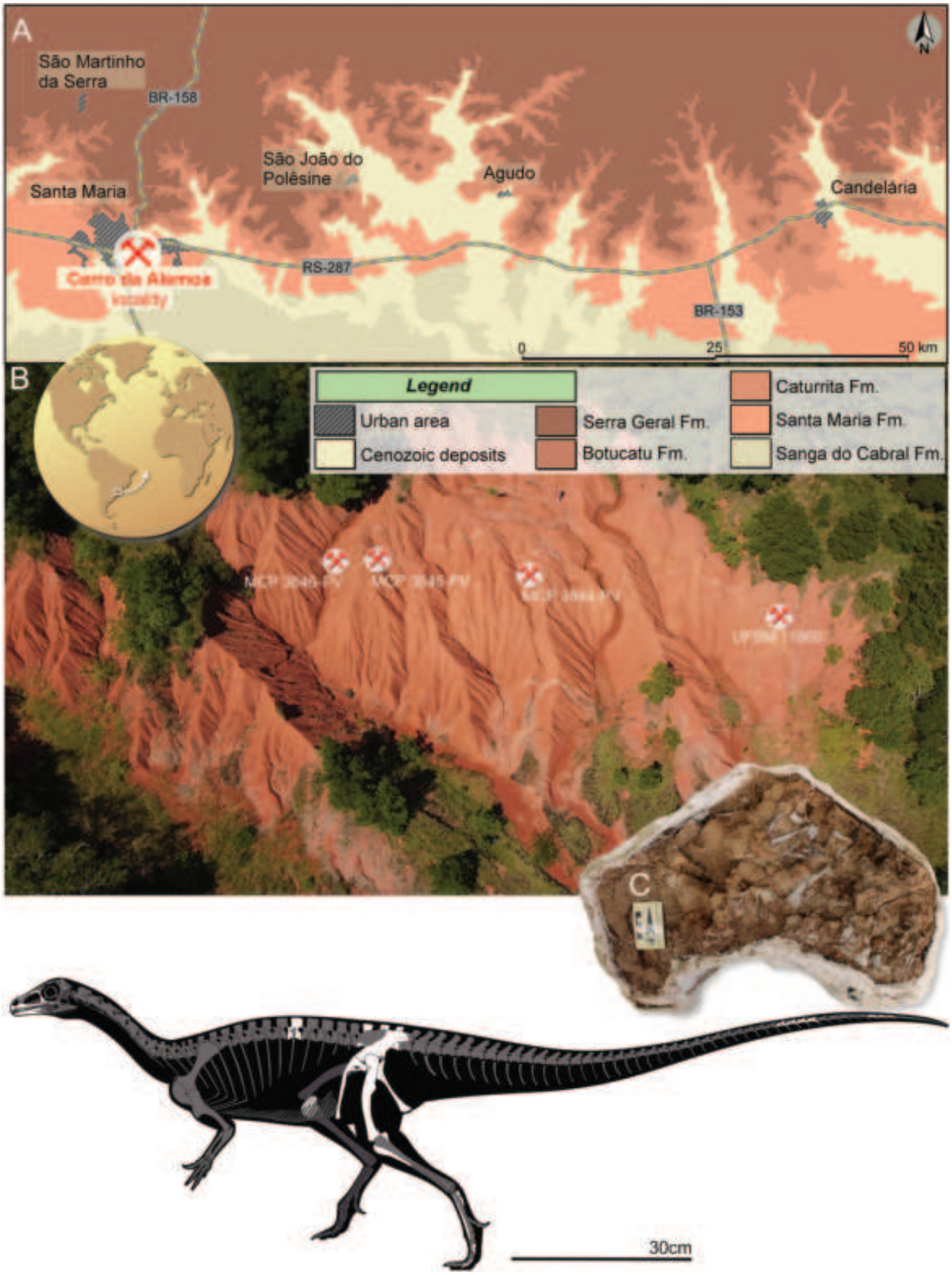

Figure 1. Study area and geological context of UFSM 11660: (A) location and geological context of Cerro da Alemoa outcrop, (B) general view of the Cerro da Alemoa outcrop, (C) plaster jacket containing the elements of UFSM 11660 partially exposed and reconstruction of preserved elements of UFSM 11660 (artwork by Maurício S. Garcia). The sites indicating where the type-specimens were found are based on the recollection of one of the authors (M.C.L.), who excavated the three specimens back in 1998; henceforth, they are not totally precise.

Table 1. Measurements employed in order to estimate skull length of UFSM 11660 and *Pampadromaeus barberenai* (ULBRA-PVT 016)

Taxa	Skull length (mm)	Maxilla length (mm)	Source
Buriolestes schultzi (CAPPA/UFSM 0035)	108.5	60	Müller *et al.* 2018a
Macrocollum itaquii (CAPPA/UFSM 001a)	147	73.1	Müller *et al.* 2020, Personal observation
Macrocollum itaquii (CAPPA/UFSM 001b)	154	72.1	Müller *et al.* 2020, Personal observation
Bagualosaurus agudoensis (UFRGS-PV-1099-T)	125.4	57.56	Pretto *et al.* 2019
Eoraptor lunensis (PVSJ 512)	123	57.11	Sereno *et al.* 2013
Plateosaurus trossingensis (SMNS 13200)	321	180	Galton 1985, Schaeffer 2024
Plateosaurus engelhardti (AMNH FABR 6810)	330	179.4	Prieto-Márquez and Norell 2011
Leyesaurus marayensis (PVSJ 706)	147.4	56.5	Apaldetti *et al.* 2011, Peyere de Fabrègues, personal observation
Pampadromaeus barberenai (ULBRA-PVT 016)	124.54[a]	57.39	Personal observation
UFSM 11660	104.37[a]	46.5	Personal observation

[a]estimated.

UFSM 11660F, proximal caudal vertebrae; UFSM 11660G, articulated caudal vertebrae; UFSM 11660H, caudalmost caudal vertebrae; UFSM 11660I, complete right femora; UFSM 11660J, proximal right femora; UFSM 11660K, proximal portion of a left tibia; UFSM 11660L, right tibia; UFSM 11660M, metatarsus I, II, III and phalange; UFSM 11660N, metatarsus I and II.

Locality and horizon

UFSM 11660 was excavated from the Cerro da Alemoa (= Waldsanga) site (Langer 2005, Da-Rosa 2015, Garcia *et al.* 2019a; 29° 41′ 51.0″ S, 53° 46′ 26.5″ W), in the municipality of Santa Maria (Fig. 1), which exposes rocks of the Candelária Sequence (Horn *et al.* 2014) of the Santa Maria Supersequence (Zerfass *et al.* 2003). The outcrop is composed of reddish mudstones, typical of the Alemoa Member of the Santa Maria Formation (Andreis *et al.* 1980). The occurrence of the rhynchosaur *Hyperodapedon* places the site in the *Hyperodapedon* Assemblage Zone (Langer *et al.* 2007a, *Schultz et al.* 2020). In addition to rhynchosaurs, it yielded dinosaur, silesaurid, lagerpetid, and cynodont remains (Langer *et al.* 1999, Martinelli *et al.* 2017, Garcia *et al.* 2019a, Marsola *et al.* 2019, Mestriner *et al.* 2023). Radioisotopic dating indicates a maximum depositional age of 233.23 ± 0.73 Mya (Langer *et al.* 2018).

Ontogenetic remarks

Bones of UFSM 11660 have some osteological indicators of skeletal maturity, such as a raised scar on the lateral surface of the dorsal portion of the iliac blade (Garcia *et al.* 2019b) and a proximal portion of the femur with a craniolateral scar, a well-developed trochanteric shelf, and a rounded dorsolateral trochanter (Piechowski *et al.* 2014, Griffin and Nesbitt 2016a, Müller 2022). In addition, all neurocentral sutures are closed (Brochu 1996, Henrich *et al.* 2021, but see Irmis 2007). Although the specimens are not skeletally immature, it is uncertain if they reached their maximum size.

DESCRIPTION AND COMPARISONS

The description followed the veterinarian anatomical terms (i.e. 'cranial'/'rostral' and 'caudal' are used rather than 'anterior' and 'posterior'), the complete list of specimens used for comparison is in Table 2 and measurements of UFSM 11660 in Table 3.

Cranial remains

The association includes one skull with articulated to partially articulated elements (Fig. 2). Hence, the following description of the rostral region, braincase, and partial lower jaws refers to a single individual. The bone surface of the elements is usually well-preserved, but the extremities of some bones are not entirely preserved.

Premaxilla: Both premaxillae are preserved, although slightly displaced from their original position (Fig. 3). The bone has a convex rostroventral margin and the narial fossa occupies the dorsal half of its main body. The right premaxilla preserved the caudolateral and medial processes, whereas only the dorsal process is present in the left bone. The anterior premaxillary foramen (*sensu* Sereno *et al.* 2013) pierces the lateral surface of the bone and an additional, smaller foramen is seen dorsal to that. The rostral tip of the left premaxilla is not preserved, exposing a tooth root. The dorsal process is short and tapers dorsally. Similarly, the caudolateral process is short, as in *Pampadromaeus barberenai* and *Bu. schultzi* (Cabreira *et al.* 2011, 2016, Müller *et al.* 2018b). On the other hand, in *E. lunensis* the process is well developed and elongated, composing the caudal margin of the external nares (Sereno *et al.* 2013). The medial process forms a thin blade and is not completely preserved. The displacement of the premaxillae prevents the defining the presence and shape of the subnarial foramen. Unlike *Bu. schultzi* (Müller *et al.* 2018b), the caudoventral corner of the bone lacks a notch forming a marked gap at the maxilla premaxilla contact. There are at least three teeth preserved in the right premaxilla and although the tooth number cannot be accessed in the left bone, it is possible to see that the first tooth starts in its rostralmost part.

Maxilla: Both maxillae are preserved, but only the left one in its full length (Figs 3, 4). The rostral process is short and its lateral surface bears some foramina. As in *Pam. barberenai*, two depressed areas excavate the medial surface of the dorsocaudally oriented dorsal process. The longitudinal ridge delimits the

Table 2. Sources of anatomical data used for comparison

Taxon	Specimen and reference
Bagualosaurus agudoensis	UFRGS-PV-1099-T (Pretto *et al.* 2019)
Buriolestes schultzi	ULBRA-PVT 280 (Cabreira *et al.* 2016) CAPPA/UFSM 0035 (Müller *et al.* 2018a) CAPPA/UFSM 0244 (Moro *et al.* 2023)
Chromogisaurus novasi	PVSJ 845 (Ezcurra 2010, Martínez *et al.* 2013)
Eoraptor lunensis	PVSJ 512 (Sereno *et al.* 2013)
Macrocollum itaquii	CAPPA/UFSM 0001a (Müller *et al.* 2018c, Müller 2020) CAPPA/UFSM 0001b (Müller *et al.* 2018c, Müller 2020)
Mbiresaurus raathi	NHMZ 2222 (Griffin *et al.* 2022) NHMZ 2547 (Griffin *et al.* 2022)
Nhandumirim waldsangae	LPRP/USP 0651 (Marsola *et al.* 2019)
Pampadromaeus barberenai	ULBRA-PVT016 (Cabreira *et al.* 2011, Langer *et al.* 2019)
Panphagia protos	PVSJ 874 (Martínez and Alcober 2009, Martínez *et al.* 2013)
Saturnalia tupiniquim	MCP 3844-PV (Langer *et al.* 1999, Langer 2003, 2007b) MCP 3845-PV MCP 3846-PV
Unaysaurus tolentinoi	UFSM 11069 (Leal *et al.* 2004)

ventral margin of the antorbital fossa, which extends along the entire length of the bone. Dorsal to that, six neurovascular foramina pierce the fossa, forming a row parallel to the alveolar margin. Unlike unaysaurids (Müller *et al.* 2018c), the rostralmost portion of the antorbital fossa lacks any evidence of a promaxillary fenestra, or of any other excavation. Both internal and external antorbital fenestrae are rostrocaudally elongated. The rounded rostroventral corner of the internal antorbital fenestra forms a straight to slightly obtuse angle (Fig. 2C). The maxillary caudal process is elongated and tapers at the distalmost portion, which has a longitudinally elongated slot on its dorsolateral margin to receive the jugal. The tooth margin is straight along its entire length and bears 19 tooth positions.

Nasal: The specimen preserves the left nasal, which is not completely preserved (Fig. 2). It corresponds to a thin blade of bone, with a dorsal recess in its lateral side. In dorsal view, the rostral process tapers medially. In lateral view, it projects ventrally to form the dorsal rim of the external nares. The lateral margin of the bone is poorly preserved. As a consequence, it is uncertain if it forms a well-projected shelf, as in other early sauropodomorphs (Martínez and Alcober 2009, Sereno *et al.* 2013, Müller *et al.* 2018a). There is no evidence of crests or ornaments on the dorsal surface of the nasal.

Lacrimal: Only the left lacrimal is preserved. It has an inverted L-shape and contributes to the dorsal and caudal margins of the antorbital fenestra (Fig. 2). The bone also contributes to the caudal margin of the antorbital fossa, which invades the ventral and anterior processes. The ventral process is slightly longer than the rostral. The lateral margin of the rostral process folds ventrally, forming a ventral crest that extends longitudinally. The lateral surface of the boundary between the rostral and ventral processes is slightly striated. Yet, this region lacks the flange present in *Bu. schultzi* (CAPPA/UFSM 0035). The ventralmost portion of the ventral process expands caudally, overlapping dorsally the rostral tip of the jugal when in articulation.

Prefrontal: The left prefrontal is disarticulated and preserves the caudal process (Fig. 2). The preserved dorsal portion is flat. The corner between the dorsal and lateral surfaces is convex in lateral view. The caudal process tappers caudally and is slightly concave in lateral view. Its general morphology resembles that of coeval sauropodomorphs (e.g. *Panphagia protos*, *S. tupiniquim*, and *Bu. schultzi*).

Frontal: The left frontal is partially preserved and longer than wide. Its ventral surface is exposed, revealing a deep fossa for the olfactory bulb. A laterally concave crest extends along the bone, separating the orbital margin and the cranial fossa, as in *S. tupiniquim* (MCP 3845-PV) and *Pam. barberenai* (Bronzati *et al.* 2019b, Langer *et al.* 2019). The crest differs from that of *Pan. protos*, which is formed by two parallel ridges (Martínez *et al.* 2013).

Jugal: The jugal is not entirely preserved (Fig. 2), lacking the caudal portion. The rostral portion of the bone is elongated and gracile, unlike the taller main body of the bone in herrerasaurs (Sereno and Novas 1993, Nesbitt *et al.* 2009, Pacheco *et al.* 2019). The rostral tip is particularly thin dorsoventrally (Fig. 4), where it articulates with the maxilla ventrally and dorsally to the lacrimal. The preserved part of the jugal has a smooth lateral surface, a sharp ventrolateral corner, and almost parallel dorsal and ventral margins. The dorsal surface is gently convex on the region that forms the ventral margin of the orbit. On the preserved caudal portion of the bone, there is a dorsal expansion (= dorsal process), which is not entirely preserved.

Braincase: Of the braincase elements, only the basioccipital, parabasisphenoid and prootic (Fig. 5) are partially exposed. A future contribution will present additional details with the aid of CT-scan data. Forming the caudal portion of the basioccipital, the occipital condyle is kidney shaped, with a more expanded and concave dorsal portion, tapering ventrally in caudal view.

Table 3. Measurements of the elements of UFSM 11600 (in mm).

Element	**Measurement**	
Skull	**Left**	**Right**
Skull length (UFSM 11660A)	104.37[b]	
Premaxilla length	11.67[a]	14.89
Premaxilla height	8.64[a]	5.21
Maxilla length	46.5	18.94[a]
Maxilla height at the base of ascending process	6.19	6.45
Antorbital fenestra length	34.16	
Antorbital fenestra maximum height	15	
Lacrimal rostral process length	11.56[a]	
Lacrimal ventral process length	15.20	
Jugal length	26.03[a]	
Frontal length	19.87[a]	
Dentary length	43.46[a]	28.98[a]
Dentary height	5.24	5.64
Dentition	Apicobasal length	Mesiodistal length
1st Premaxillary tooth	6.56	3.31
2nd Premaxillary tooth	5.51	3.09
3rd Premaxillary tooth	5.49	2.91
1st Maxillary tooth	6.11	3.60
2st Maxillary tooth	4.99	3.26
18th Maxillary tooth	2.36	1.92
5th Dentary tooth	4.65	2.36
Axial series	Length	
Dorsal centrum UFSM 11660B	22.37	
Dorsal centrum UFSM 11660B	23.46	
Dorsal centrum UFSM 11660B	23.48	
1st Sacral centrum UFSM 11660C	18.47	
2nd Sacral centrum UFSM 11660C	19.30	
1st Sacral centrum UFSM 11660D	19.30[a]	
2nd Sacral centrum UFSM 11660D	21.32	
1st Sacral centrum UFSM 11660E		
2nd Sacral centrum UFSM 11660E		
1st Caudal centrum UFSM 11660F	17.14	
2nd Caudal centrum UFSM 11660F	17.15	
3rd Caudal centrum UFSM 11660F	17.93	
4th Caudal centrum UFSM 11660F	18.69	
5th Caudal centrum UFSM 11660F	11.33[a]	
6th Caudal centrum UFSM 11660F	16.39	
7th Caudal centrum UFSM 11660G	14.36[a]	
8th Caudal centrum UFSM 11660G	20.18	
9th Caudal centrum UFSM 11660G	20.18	
10th Caudal centrum UFSM 11660G	19.58	
11st Caudal centrum UFSM 11660G	18.03	
12nd Caudal centrum UFSM 11660G	19.23	
13rd Caudal centrum UFSM 11660G	19.24	
14th Caudal centrum UFSM 11660G	18[a]	
15th Caudal centrum UFSM 11660H	14.69	
16th Caudal centrum UFSM 11660H	14.70	
17th Caudal centrum UFSM 11660H	11.92	
18th Caudal centrum UFSM 11660H	12.36	

Table 3. Continued

Element	Measurement	
	Left	**Right**
Hind limb	Left	Right
Ilium pubic peduncle to ala postacetabular (length) UFSM 11660C	88.71	
Ilium acetabulum length UFSM 11660C	29.54	
Ilium acetabulum height UFSM 11660C	23.37[a]	
Pubis length UFSM 11660C	117.38	49.17[a]
Ischium length UFSM 11660C	102.40	
Ischium proximal width UFSM 11660C	14.08	
Ischium proximal length UFSM 11660C	24.77	
Ischium distal width UFSM 11660C	10.55	
Ischium distal length UFSM 11660C	16.39	
Femur length UFSM 11660I		157
Femur head longer length UFSM 11660I		29.97
Femur head shortest UFSM 11660I		16.27
Femur distal craniocaudal width (with crista tibiofibularis) UFSM 11660I		24.86
Femur distal mediolateral width UFSM 11660I		30.38
Circumference UFSM 11660I		49.18
Femur length UFSM 11660J		54.85[a]
Femur head longer length UFSM 11660J		27.89
Femur head shortest length UFSM 11660J		18.80
Circumference UFSM 11660J		53
Tibia length UFSM 11660K	71.94[a]	
Tibia proximal craniocaudal length UFSM 11660K	27.45	
Tibia proximal lateromedial length UFSM 11660K	20.80	
Tibia length UFSM 11660L		36.81[a]
Tibia proximal craniocaudal length UFSM 11660L		30.32[a]
Tibia proximal lateromedial length UFSM 11660L		20.11[a]
Metatarsal I length UFSM 11660M		47.44
Metatarsal II length UFSM 11660M		49.31[a]
Metatarsal III length UFSM 11660M		68.20
Metatarsal II length UFSM 11660N		36.17[a]
Metatarsal III length UFSM 11660N		76.32

[a]Incomplete.
[b]Estimate.

The main body of the parabasisphenoid is preserved, with the basipterygoid process, projecting cranioventrally as in a paratype of *S. tupiniquim* (MCP 3845-PV; Bronzati *et al.* 2019a), but not laterally as in *Bu. schultzi* (CAPPA/UFSM 0035; Müller *et al.* 2020). The pituitary fossa excavates the rostral surface of the main body of the bone, in the same craniocaudal level of the basipterygoid process. The fossa is relatively short, resembling the condition of *Bu. schultzi* (CAPPA/UFSM 0035; Müller *et al.* 2020) and differing from the enlarged fossa of latter sauropodomorphs (Carabajal 2012). There are two foramina interpreted as the path of the internal carotid foramina, they are in a position similar to that seen in a paratype of *S. tupiniquim* (MCP 3845-PV; Bronzati *et al.* 2019a). Dorsally to the parabasisphenoid, the prootic is preserved. Additionally, it is possible to observe the floccular fossa in cross-section.

Dentary: Both dentaries are partially preserved (Figs 2–4). The bone is relatively slender, unlike the robust dentary of latter sauropodomorphs. The dorsal margin of its rostral end is ventrally deflected, such as in other early sauropodomorphs (Matínez and Alcober 2009, Sereno *et al.* 2013, Cabreira *et al.* 2016, Müller *et al.* 2018a, Langer *et al.* 2019). On the contrary, the ventral margin is straight, differing from the ventrally directed margin of taxa like *Unaysaurus tolentinoi* (Leal *et al.* 2004). The lateral surface of the dentary is pierced by a series of foramina, which starts at the rostralmost portion of the bone and extends caudally as in *Pan. protos*, *Bu. schultzi*, and *Bagualosaurus agudoensis*. In contrast, there is a gap between the first and the next foramen, as in *Pam. barberenai*. In medial view, the Meckelian groove excavates the ventral portion of the bone, as in *Pan. protos*. The first alveolus is inset 2.4 mm from the rostralmost end of the bone. The rostralmost teeth are slightly rostrally inclined relative to the

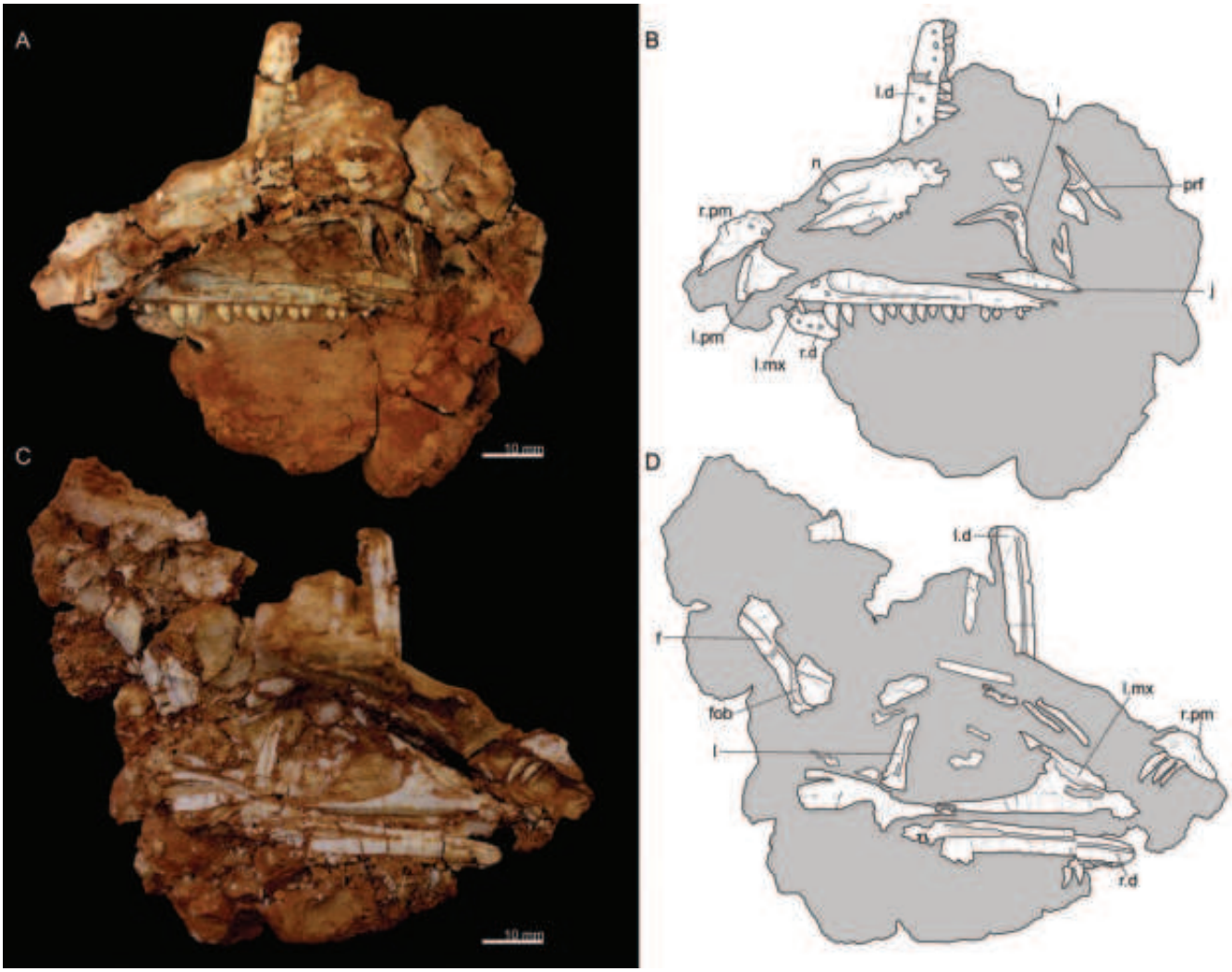

Figure 2. Skull of UFSM 11660A: (A, B) lateral and (C, D) medial views. Abbreviations: d, dentary; fob, fossa for the olfactory bulb; j, jugal; l, lacrimal; mx, maxilla; n, nasal; pm, premaxilla; prf, prefrontal. l. left and r. right.

alveolar margin. The mandibular symphysis is short, restricted to the rostral end of the dentary. In medial view, it is possible to identify the interdental plates, which are triangular. The posterior portion of both dentaries is poorly preserved.

Dentition: UFSM 11660A bears typical ziphodont teeth, resembling the condition of other early sauropodomorphs, such as *E. lunensis* (Sereno *et al.* 2013) and *Bu. schultzi* (Cabreira *et al.* 2016, Müller *et al.* 2018a, Moro *et al.* 2024). The right premaxilla preserves three teeth caudal to an empty tooth position (Fig. 3). The apicobasal length of the first preserved crown (second premaxillary tooth) is 7 mm. All teeth lack basal constrictions. The second tooth has serrations (eight per millimetre) only in the mesial margin. These are also seen in the distal margin of the 2nd (CAPPA/UFSM 0244) (Müller *et al.* 2018a, Moro *et al.* 2024) and 3rd (CAPPA/UFSM 0035) premaxillary teeth of *Bu. schultzi*, whereas *Pam. barberenai* has serrations in both carinae of the 4th and in the distal carina of the 3rd premaxillary tooth (Langer *et al.* 2019). The premaxillary teeth are longer and thinner than those of the maxilla (Table 3).

In the maxilla, UFSM 11660A has at least 19 tooth positions (Fig. 4), whereas *Bu. schultzi* has 24, *Pam. barberenai* has 21, and *Ba. agudoensis* 23. In labial/lingual views, the mesial margin of the rostral teeth is slightly convex and the distal is almost straight, resulting in a blade-like shape. In more caudal teeth, both margins are slightly convex. The longer tooth crown is 5.5 mm in apicobasal length and the smaller is 2.7 mm. The wider crown is 3.07 mm in mesiodistal width, whereas the smaller is 1.5 mm. The teeth bear ~8 serrations per millimetre. The number of dentary teeth cannot be defined, as the bone is not complete (Fig. 4). The apical parts of the rostral teeth are broken. The 5th tooth has the mesial margin convex and the distal one almost straight in labial/lingual views.

Axial remains

The preserved axial elements of UFSM 11660 include at least three dorsal vertebrae, three sets of sacral vertebrae, and 18 caudal vertebrae, only some of them partially articulated. One of the sets of sacral vertebrae is quite damaged, hampering mechanical preparation and, consequently, reliable observations. Due to

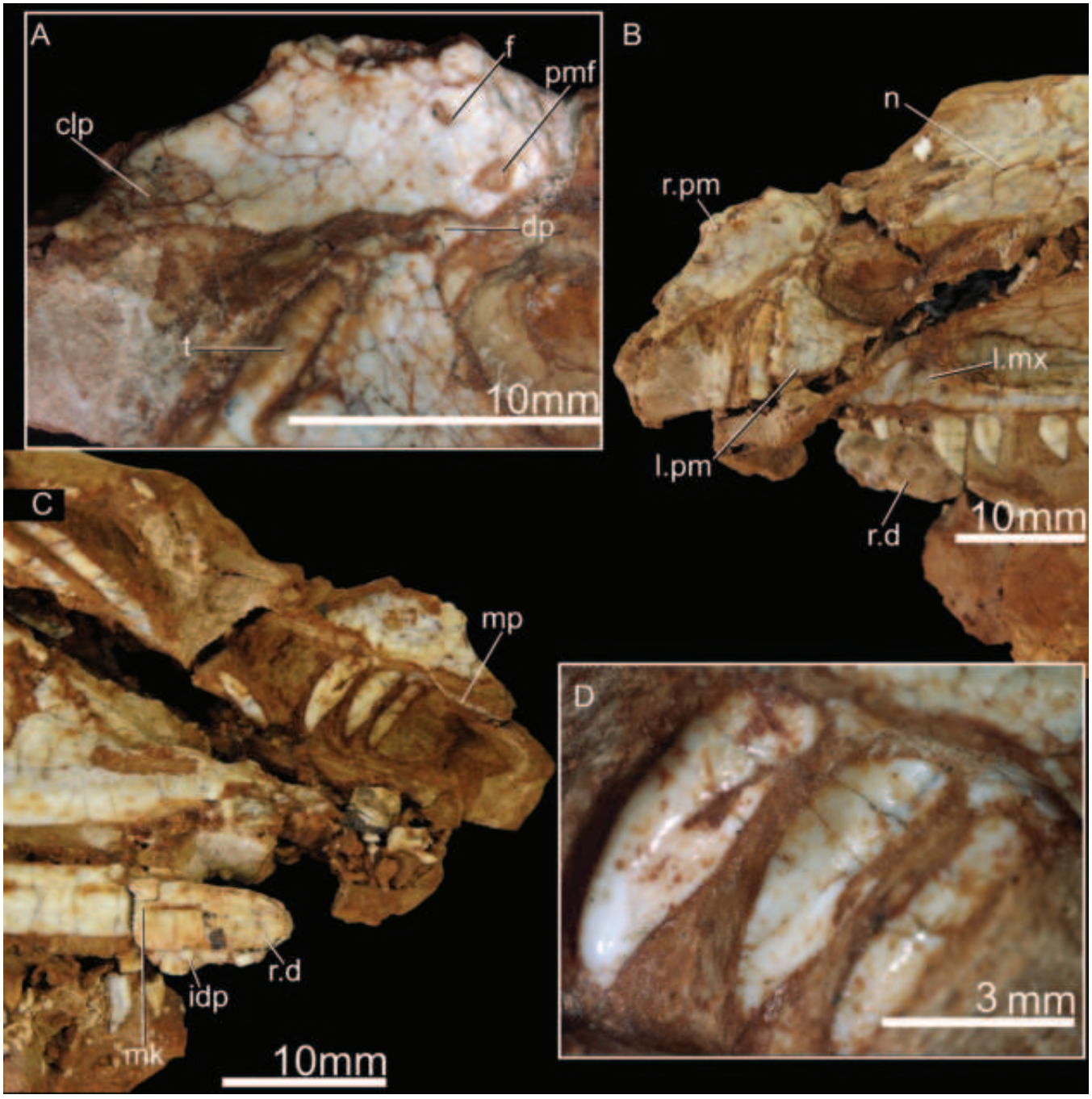

Figure 3. Premaxilla and maxilla of UFSM 11660A: (A, B) lateral and (C, D) medial views. Abbreviations: clp, caudolateral process; dp, dorsal process; f, foramen; idp, interdental plate; l.mx, left maxilla; mk, Meckelian groove; mp, medial process; n, nasal; r.d, right dentary; pm, premaxilla; pmf, premaxillary foramen; t, tooth.

the impossibility to assign the vertebrae to specific individuals, they are described below simply according to their position on the axial series.

Dorsal vertebrae: UFSM 11660B includes three dorsal vertebrae, two of which in articulation (Fig. 6). The centra are longer (2.3 mm) than tall (1.4 mm) and lack a ventral keel. Both articular facets are concave and almost as tall as wide. Their parapophysis are located above the centrum, contacting the diapophysis, so the elements are considered as part of the caudal half of the series (Sereno *et al.* 2013, Müller *et al.* 2018a, Langer *et al.* 2019). Neurocentral sutures are observed in all vertebrae and a slight depression is seen on the lateral surface of their centra. In the neural arches, the diapophyses are dorsolaterally oriented and subretanctangular in dorsal view. The neural spines are caudally inclined and lack any evidence of spine tables. Pre- and postzigapophyses are broken.

Sacral vertebrae: The two best-preserved sets are composed of two articulated primordial sacral vertebrae. UFSM 11660C is

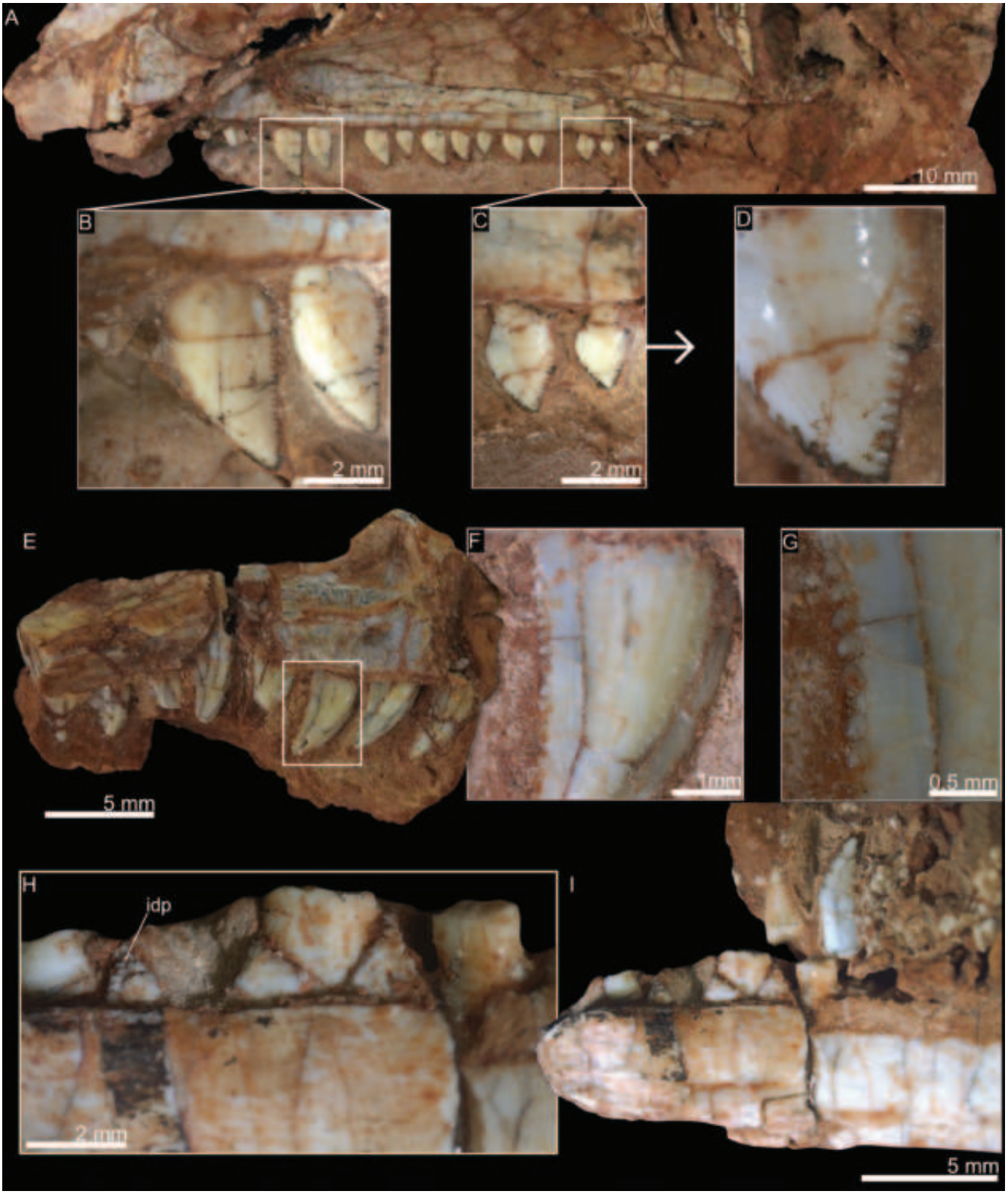

Figure 4. Dentition of UFSM 11660A: (A) overview of the left maxilla in lateral view; (B, C, D) maxillary teeth in labial view, (E) right maxilla in lateral view, (F) anterior maxillary teeth in labial view, (G) magnification of the anterior maxillary teeth, (H) interdental plates of the dentary, and (I) right dentary in medial view. Abbreviations: idp, interdental plates.

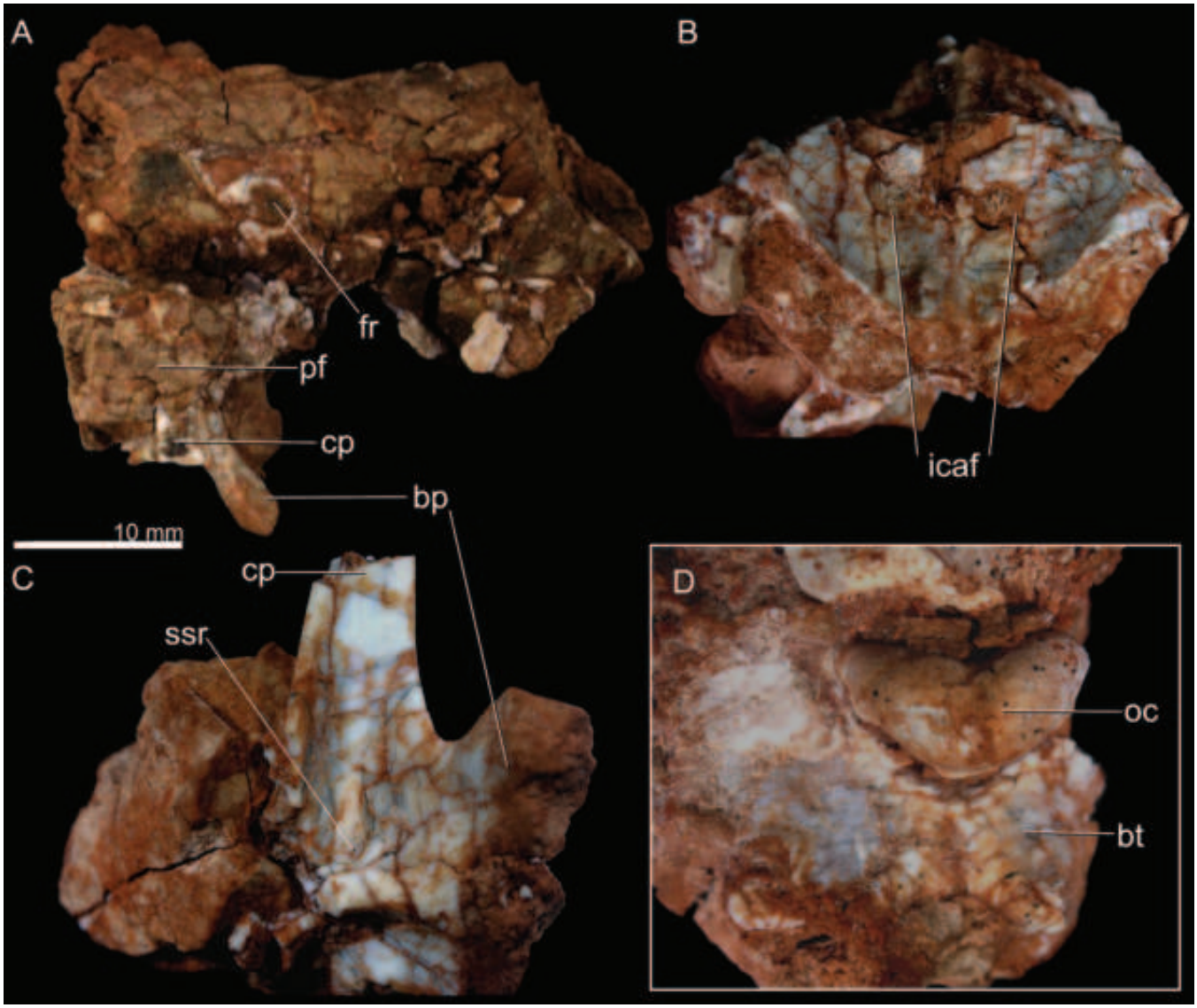

Figure 5. Braincase elements of UFSM 11660A: (A) cranial, (B) dorsal, (C) ventral, and (D) caudal views. Abbreviations: bt, basal tubera; bp, basipterygoid process; cp, cultriform process; fr, floccular recess; icaf, foramina for the internal carotid artery; oc, occipital condyle; pf, pituitary fossa; ssr, subsellar recess.

articulated with the ilium and UFSM 11660D is isolated (Fig. 7). The centra of UFSM 11660D are slightly wider lateromedially and shallower dorsoventrally than those of UFSM 11660C. In UFSM 11660C, the S1 cranial articular surface is concave. In both sets, the S2 caudal articular surface is concave and almost as wide as deep. The sacral centra are not co-osified in both sets and lack ventral keel.

In UFSM 11660C, sacral ribs and transverse processes form a single structure, which connects to the ilium. In UFSM 11660D, in lateral view, the first sacral rib and transverse process form a C-shape, whereas the S2 rib is S-shaped. The neural spines of UFSM 11660C are dorsocaudally inclined, but this might be affected by taphonomy. The prezygapophysis of UFSM 11660C is rounded and projects craniodorsally. In dorsal view of both sets, the transverse processes of S1 and S2 do not contact one another. The S1 transverse process of UFSM 11660D is wider, exhibiting a fan shape. The S2 transverse process is laterocaudally oriented in both sets.

Caudal series: The caudal series is composed of 18 vertebrae (Fig. 8), including an articulated set of eight mid-caudal vertebrae with chevrons (UFSM 11660G), and ten disarticulated elements, six located proximal (UFSM 11660F) and four distal (UFSM 11660H) to the articulates segment. The centra become longer in the direction to the distal portion of the tail. None of the caudal centra has a ventral keel and both their articular facets are concave.

The six proximalmost vertebrae (UFSM 11660F) are axially shortened, with their transverse processes dorsolaterally oriented. The prezygapophysis projects craniodorsally, whereas the postzigapophysis projects caudoventrally. The eight articulated vertebrae (UFSM 11660G) have centra longer than deep, the ventral surface of which lacks a keel. The transverse process is thin and the neural spine is low. The prezygapophysis is craniodorsally inclined, with a rounded and elongated articular facet. The postzygapophysis are rounded. The distalmost vertebrae (UFSM 11660H) are very elongated. These elements are proportionally smaller and do not preserve neural arches.

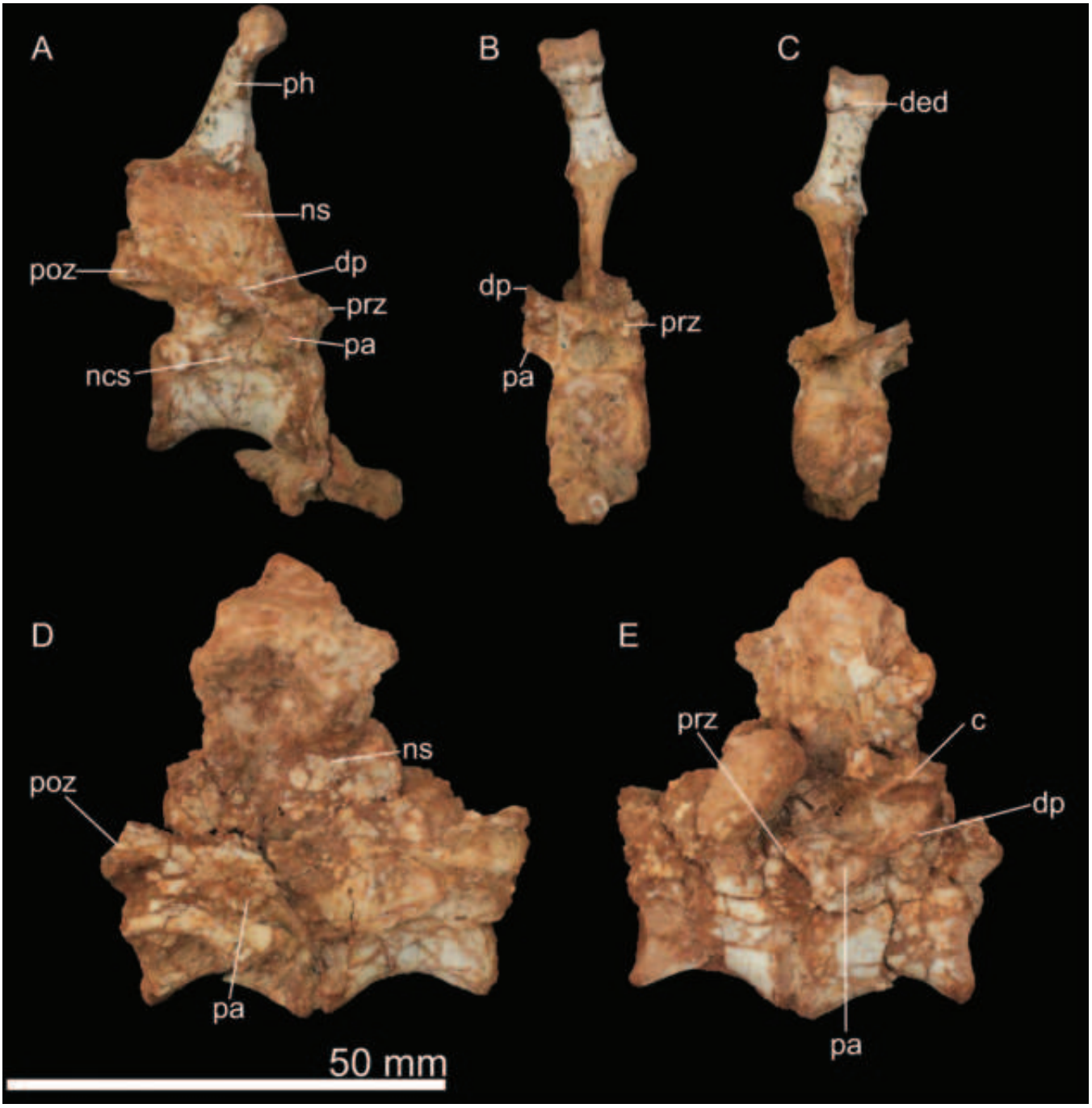

Figure 6. Dorsal vertebrae of UFSM 11660B: (A, D, E) Lateral, (B) cranial, and (C) caudal views. Abbreviations: c, centra; ded, dorsal extensor depression; dp, diapophysis; ncs, neurocentral; ns, neural spine; pa, parapophysis; ph, phalange; poz, postzygapophysis; prz, prezygapophysis.

Pelvic girdle and hindlimb

Ilium: One partial ilium is preserved with sacral vertebrae in the association UFSM 11660C (Fig. 9). It is almost complete, lacking the preacetabular ala and part of the iliac blade. A disarticulated caudal vertebra is attached to the acetabular wall.

The postacetabular ala is elongated, unlike that of herrerasaurids. There is a conspicuous rugose area on the lateral surface of this structure, identified as the origin of the flexor tibialis externus (Langer 2003). The brevis shelf delimits the brevis fossa, but does not connect to the supracetabular crest. The supracetabular crest is lateroventrally oriented, its maximum width is at the centre of the acetabulum, and it does not reach the distal end of the pubic peduncle. The acetabular wall of the ilium is not perforated and its ventral margin is straight to slightly concave. The pubic peduncle is cranioventrally directed and its extremity has a subtriangular distal outline. The ischiadic peduncle is ventrally directed. It has an ovoid distal outline and lacks a heel-like projection on the caudal margin.

Pubis: The pair of partially articulated pubis (UFSM 11660C; Fig. 10) are assigned to a single individual. The most complete

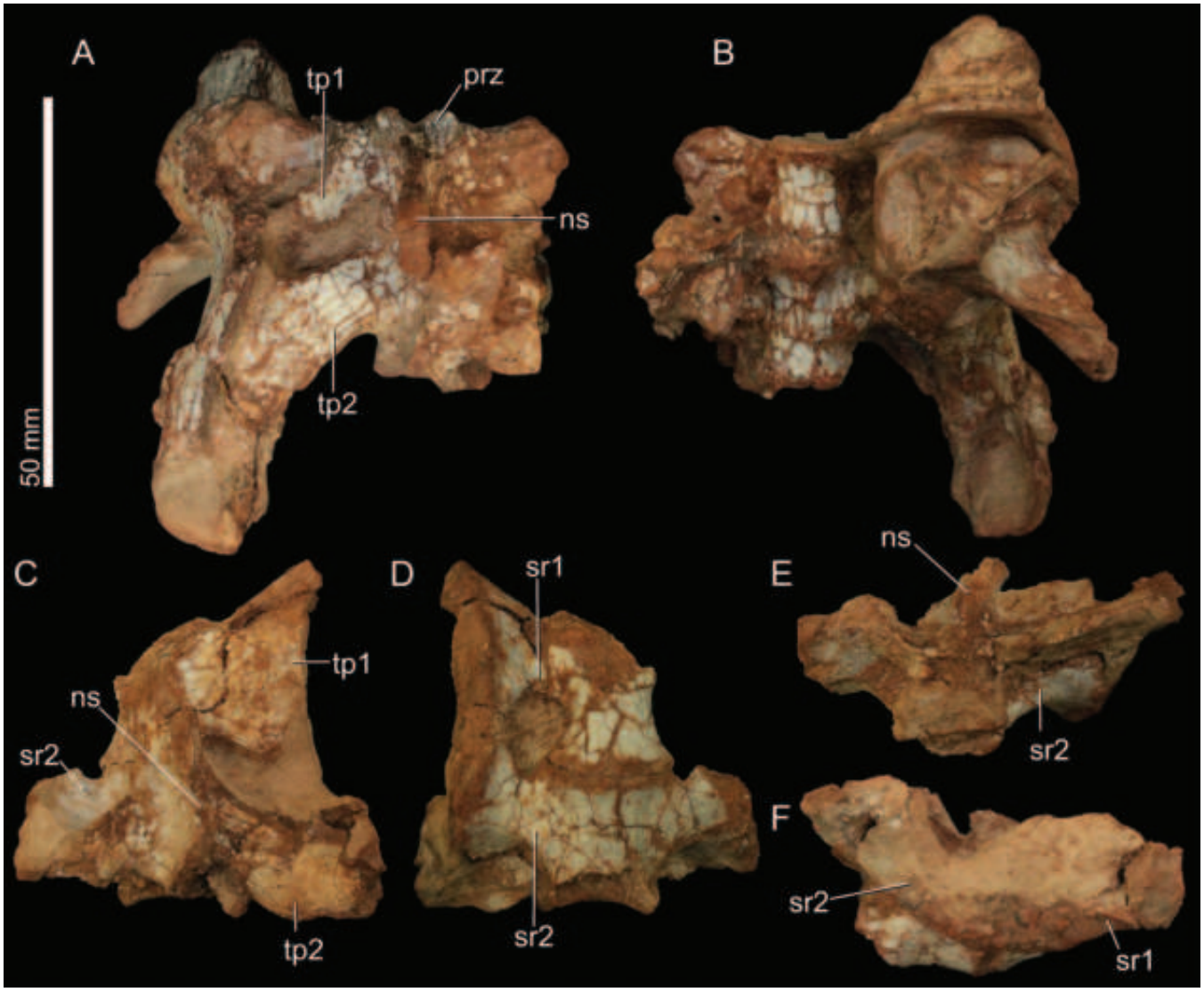

Figure 7. Sacral vertebrae of UFSM 11660C (A, B) and UFSM 11660D (C–F): (A, C) dorsal, (B, D) ventral, (E) caudal, and (F) lateral views. Abbreviations: ns, neural spine; prz, prezygapophysis; sr, sacral rib; tp, transverse process; 1, first primordial sacral vertebra; 2, second primordial sacral vertebra.

left bone is 117.38 mm long, with the main axis caudodorsally to cranioventrally oriented. The proximal outline of the iliac peduncle is rounded and the ambiens process forms a raised protuberance on the lateral surface of the main body of the bone. The shaft encompasses a thin medial lamina and its distal end expands dorsoventrally, but not as much as in herrerasaurids or theropods (Novas 1994).

Ischium: A single left ischium (UFSM 11660C) was preserved. It is *c.* 100 mm long and almost complete, lacking only part of the obturator plate. Its main body is subtriangular in lateral/medial views and the shaft is elongated, expanding dorsoventrally at the distal end (Fig. 11). The main proximal articulation (for the ilium and femur) has an ovoid outline, and the lateral (antitrochanteric) margin is convex, whereas the medial is straight to convex. The angle formed between the dorsal margin of the ischial body and the ischial shaft is more acute in UFSM 11660C, *Bu. schultzi* (ULBRA-PVT 280), other specimens of *S. tupiniquim*, and *Mbiresaurus raathi*, than in *Pan. protos*.

The antitrochanter is well-expanded laterally, so that its transition to the main body is concave (proximodistally) and well-marked in the lateral surface of the bone. At the dorsal surface of the ischium, a groove extends from near the proximal articulation until the distal end of the bone. Another longitudinal groove extends along the medial surface of the ischial shaft, as also seen in other specimens of *S. tupiniquim* (Langer 2003). A distinct protuberance is seen on the laterodorsal margin of the distal half of the shaft, which is less developed in the other specimens of *S. tupiniquim*. The distal end expands dorsoventrally and has a convex margin in lateral view. The distal outline of the bone is semi-circular, resembling the condition in *Pan. protos*.

Femur: There are two right femora in the association (Fig. 12): one almost complete (UFSM 11660I), 157 mm long, and one preserving only the proximal part (UFSM 11660J), *c.* 55 mm long as preserved. UFSM 11660I is sigmoid in cranial/caudal and lateral/medial views. Its proximal portion is poorly preserved. The craniomedial tuber is reduced and the craniolateral

Figure 8. Caudal vertebrae of UFSM 11660F (A–K), UFSM 11660G (L–M), and UFSM 11660H (N–P): (A–B, G–P) lateral, (C) cranial, (D) caudal, (E) dorsal, and (F) ventral views. Abbreviations: ch, chevron; ns, neural spine; poz, postzygapophysis; prz, prezygapophysis; tp, transverse process.

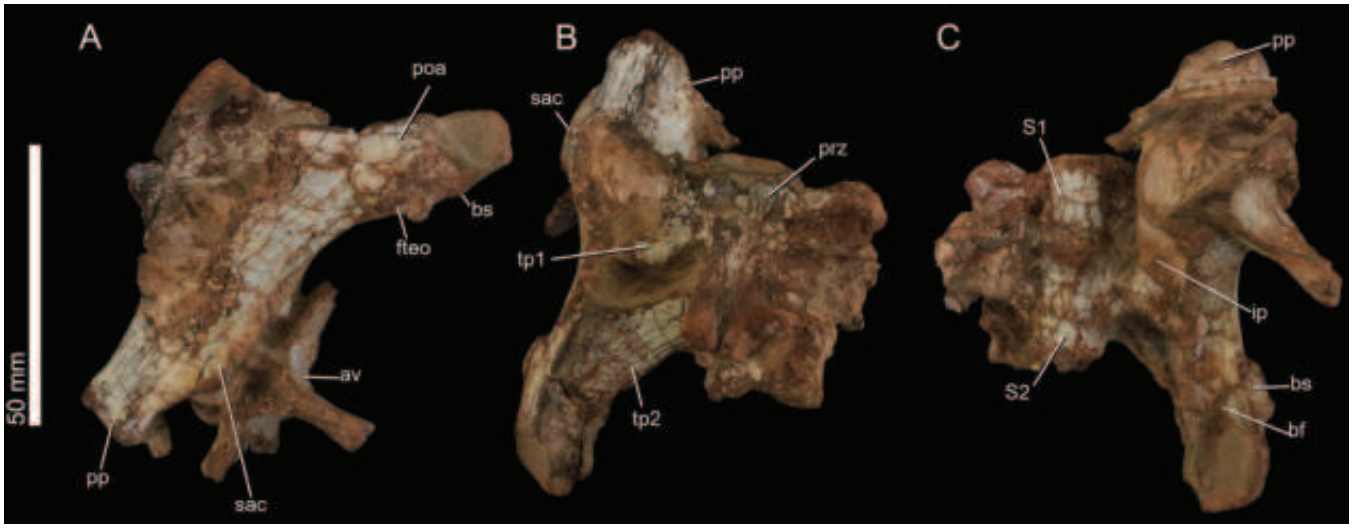

Figure 9. Ilium of UFSM 11660C: (A) lateral, (B) dorsal, and (C) ventral views. Abbreviations: av, attached vertebra; bf, fossa brevis; bs, brevis shelf; fteo, flexor tibialis externus origin; ip, ischiatic peduncle; poa, postacetabular ala; pp, pubic peduncle; prz, prezygapophysis; S1, first primordial sacral vertebra 1; S2, second primordial sacral vertebra; sac, supra-acetabular crest; tp, transverse process.

Figure 10. Pubis of UFSM 11660C: (A) cranial, (B) lateral, (C) caudal, and (D) distal views. Abbreviations: ap, ambiens process; ed, expanded distal; ml, medial lamina; r, rib; s, striated surface.

is connected to a well-developed craniomedial crest ('cmc' in Fig. 12) that extends distally along the proximal portion of the bone.

The far better-preserved femoral head of UFSM 11660J has a transverse groove on its proximal surface. The craniolateral tuber is poorly developed and connects to the craniomedial

Figure 11. Left ischium of UFSM 11660C: (A) lateral, (B) medial, (C) dorsal, (D) proximal, and (E) distal views. Abbreviations: at, antitrochanter; bp, bump; ls, lateral surface; ms, medial surface; obp, obturator plate area; rd, ridge.

crest (*sensu* Bittencourt and Kellner 2009), which extends distally along the cranial surface of the bone. The craniomedial tuber is the largest of the femoral head tubers and is separated from the caudomedial tuber by the sulcus for the capitis femoris ligament. Lateral to the caudomedial tuber, the facies articularis antitrochanterica slopes distally.

In both femora the dorsolateral trochanter forms a protuberance located at the level of the femoral head, with its cranial and lateral surfaces covered by striations. The craniolateral scar, located between the dorsolateral trochanter and the craniomedial crest is faint in UFSM 11660J, but well-marked in UFSM 11660I. In UFSM 11660J, the cranial (= lesser) trochanter forms a proximodistally oriented small prominence, the proximal tip of which is completely connected to the shaft. The distal portion of the cranial trochanter is continuous to the femoral cranial intermuscular line, as seen in craniomedial view (Langer 2003). The trochanteric shelf is set distal to the dorsolateral trochanter and corresponds to a rugose area connected to the cranial trochanter. This part of the femur is fractured in UFSM 11660I, hampering reliable observations of those elements.

Only the proximal tip of the UFSM 11660J fourth trochanter is preserved. In UFSM 11660I, it is located in the caudomedial surface of the bone and merges gently with the shaft proximally. In *Bu. schultzi*, *Mbiresaurus raathi*, *Pam. barberenai*, and other specimens of *S. tupiniquim*, the distal portion of the fourth trochanter is acute, forming an asymmetrical structure. Instead, in UFSM 11660I, the distal portion of the fourth trochanter merges smoothly to the shaft, forming a symmetrical structure. However, this area is damaged and we interpret it as a taphonomic feature. A fossa for the m. caudofemoralis longus (Langer 2003) excavates the medial surface of the femoral shaft right cranial to the fourth trochanter.

In cranial view, the distal end of the femur preserves a rugose area towards its lateral portion. The popliteal fossa marks the caudal surface of the distal portion of the bone. Its distal portion is well-delimited, but the proximal portion merges smoothly with the shaft. The distal articulation is composed of three main structures: the lateral and medial condyles and the crista tibiofibularis. A distal groove separates the lateral condyle and crista tibiofibularis. The latter is the smallest of the three structures and projects

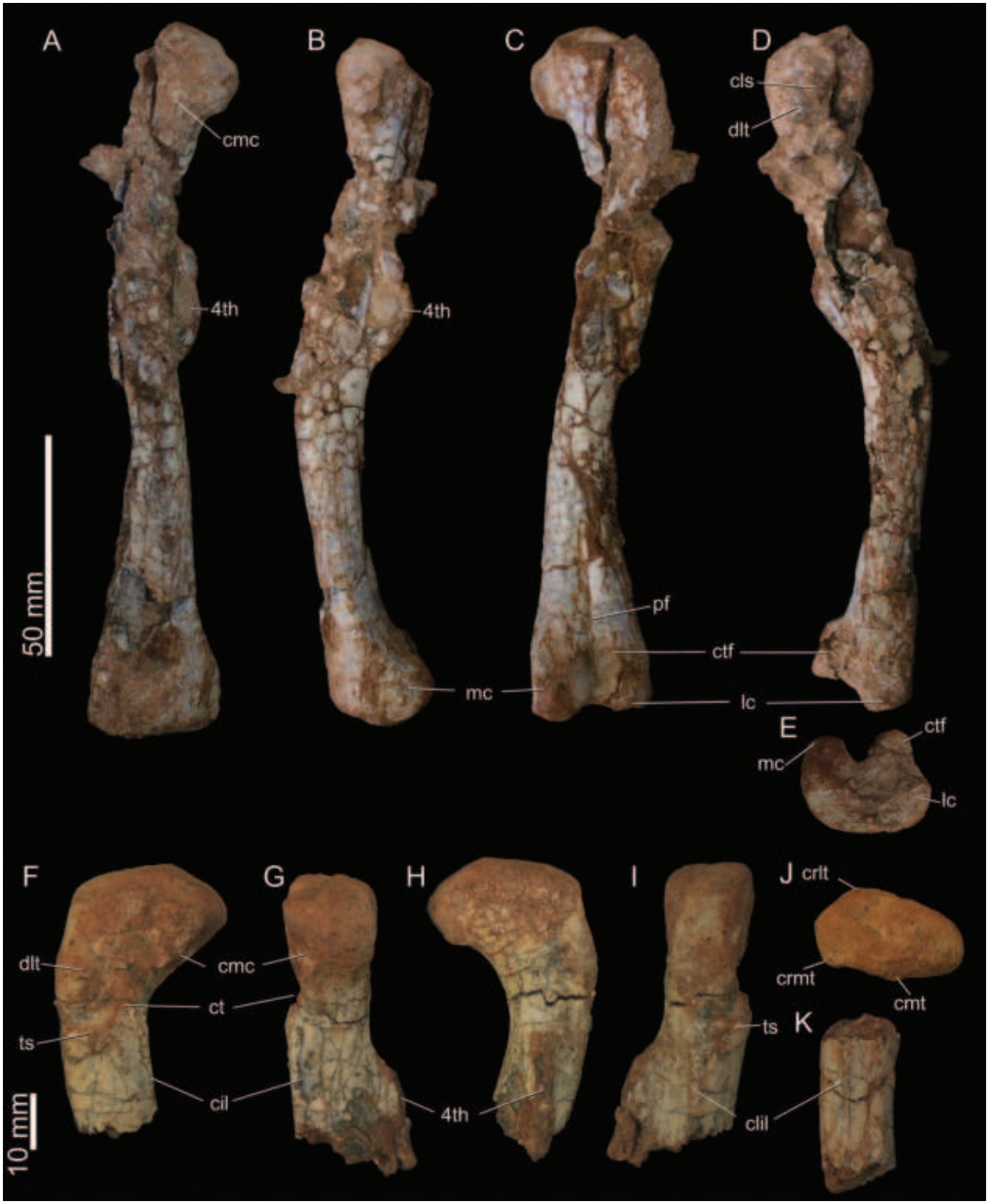

Figure 12. Right femora of UFSM 11660I (A–E) and UFSM 11660J (F–K): (A, F) cranial, (B, G) medial, (C, H) caudal, (D, I, K) lateral, (E) distal, and (J) proximal views. Abbreviations: 4th, fourth trochanter; cmt, caudomedial tuber; crlt, craniolateral tuber; crmt, craniomedial tuber; cil, cranial intermuscular line; clil, caudolateral intermuscular line; cls, craniolateral scar; cmc, craniomedial crest; ct, cranial trochanter; ctf, crista tibiofibularis; dlt, dorsolateral trochanter; lc, lateral condyle; mc, medial condyle; pf, popliteal fossa; ts, trochanteric shelf.

caudally forming a rounded tip. In distal view, the craniomedial margin of the bone is rounded, whereas that of *E. lunensis* is more projected and almost rectangular. Compared to *Mbiresaurus raathi* and some specimens of both *S. tupiniquim* (MCP 3844-PV) and *Bu. schultzi* (CAPPA/UFSM 0035), the distal end of the femur is more mediolaterally expanded in UFSM 11660I, as in other specimens of the latter taxon (ULBRA-PVT 280).

A fragmentary shaft was associated with the proximal portion of UFSM 11660J. Although they do not perfectly fit, both elements are equivalent in size. The segment is 31.61 mm long, the minimum shaft circumference is 42.97 mm, and the bone wall is 3.98 mm thick. Both caudolateral and cranial intermuscular lines are present and well developed.

Tibia: UFSM 11660 includes a pair of left/right partial tibiae with their proximal portions preserved, but it is not possible to assume that they belong to the same individual (Fig. 13). The left bone (UFSM 11660K) is better preserved and 71.94 mm long, whereas the right one (UFSM 11660L) is 'swollen' and 36.81 mm in length. Their general anatomy resembles that of early sauropodomorphs tibiae, including *Pan. protos*, *E. lunensis*, and other specimens of *S. tupiniquim*.

In proximal view, UFSM 11660K has a subtriangular shape, comprising the cnemial crest, and medial, and lateral condyles. The cnemial crest arcs craniolaterally and is rugose on its cranial surface. The medial condyle is more expanded than the lateral and a cleft/notch is seen between them as in *E. lunensis* and other

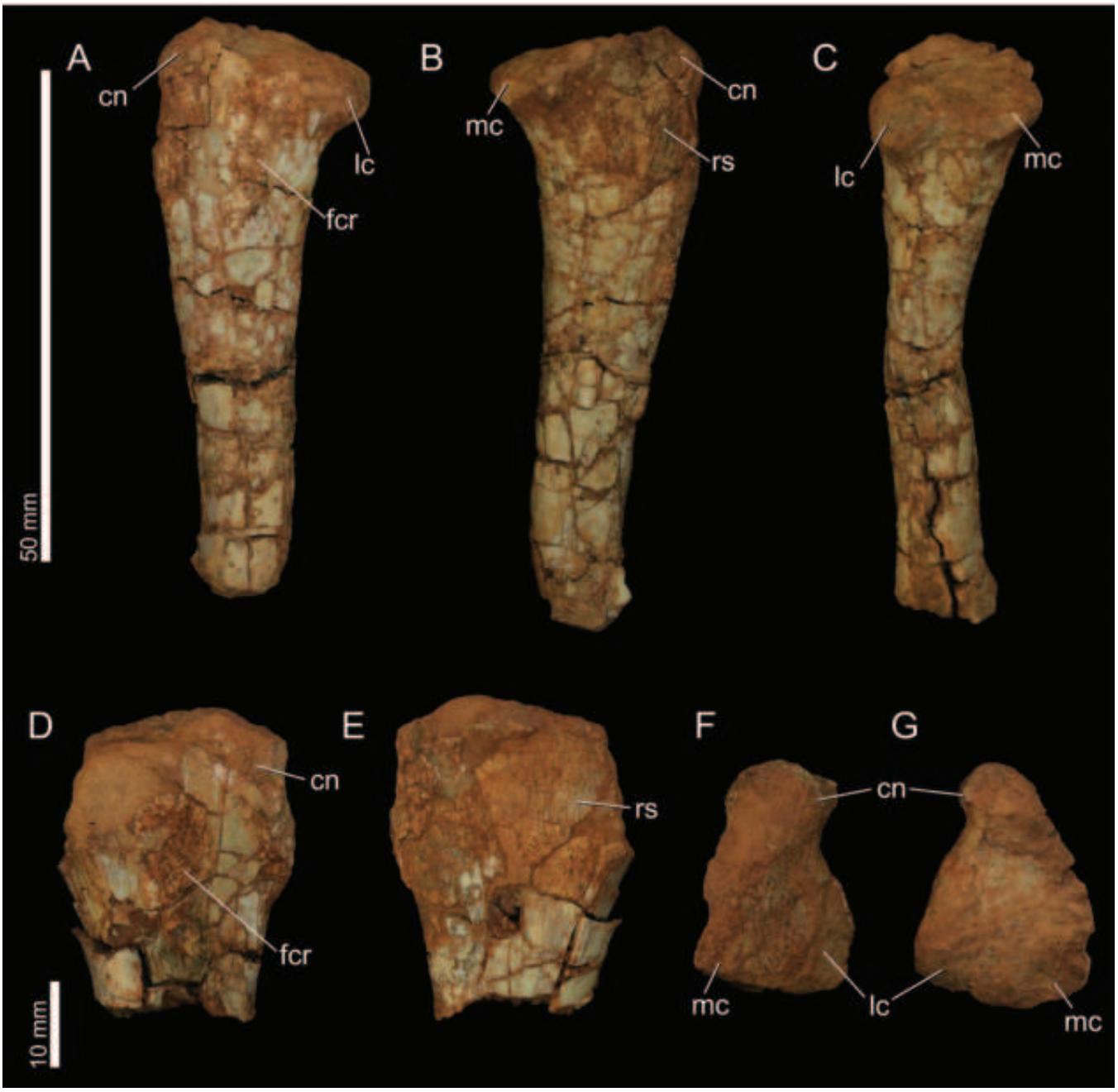

Figure 13. Tibiae of UFSM 11660K (A–C, G; left) and UFSM 11660L (D–F; right): (A, D) lateral, (B, E) medial, (C) caudal, and (F–G) proximal views. Abbreviations: cn, cnemial crest; fcr, fibular crest; lc, lateral condyle; mc, medial condyle; rs, rugose surface.

specimens of *S. tupiniquim*. Unlike *Bu. schultzi* (ULBRA-PVT 280), the medial condyle lacks a caudal projection in UFSM 11660K. The condyles and the cnemial crest are poorly preserved in UFSM 11660L, but the latter is less arched than in the left tibia.

An excavated area for the articulation with the fibula is observed in the lateral surface of both tibiae. In UFSM 11660K it starts at the level of cnemial crest and extends for 17.35 mm distally. A fibular crest extends caudally to its depression, as seen in *E. lunensis*, *Mbiresaurus raathi*, and other specimens of *S. tupiniquim*. There is a rugose area on the medial surface of the tibiae, as observed in many sauropodomorphs (e.g. *S. tupiniquim*, *E. lunensis*).

Metatarsals and phalanges: The preserved pedal parts include two sets of right metatarsals with similar morphology (Fig. 14). UFSM 11660M is slightly smaller, comprising metatarsals I, II, and III. UFSM 11660N comprises longer metatarsals II (lacking the diaphysis) and III.

The proximal portion of metatarsal I is lateromedially compressed. The bone expands distally, as the shaft arcs medially. This resembles the general morphology seen in the metatarsal I of other *S. tupiniquim* specimens. Yet, its proximal portion is not 'L-shaped' as in *Pam. barberenai* (Langer *et al.* 2019).

The metatarsal II of UFSM 11660M lacks the proximal portion, but in UFSM 11660N the bone has a subrectangular proximal outline. At the distal end, the medial condyle projects more distally in both specimens. Unlike in *Chromogisaurus novasi* (Martínez *et al.* 2013), the distal condyles are symmetrical.

The proximal outline of metatarsal III is subtriangular in both individuals, but it is more lateromedially compressed in

Figure 14. Right pes of UFSM 11660M (A–D, G–H) and UFSM 11660N (E–F): (A, E) metatarsal III in proximal (top), anterior (middle), distal (bottom) views; (B, F) metatarsal II in proximal (top), anterior (middle), distal (bottom) views; (C) metatarsal I in lateral and (D) medial views; (G–H) phalanx in lateral view. Abbreviations: a.mt, articulates with metatarsal; clp, collateral ligament; ed, extensor depressions; rdg, ridge.

UFSM 11660M. The outlines resemble those of other specimens of *S. tupiniquim*, differing from the parallelogram shape outlines of *Pan. protos* and *E. lunensis* (Martinez and Alcober 2009, Sereno *et al.* 2013). The distal articulation has the medial condyle slightly displaced medially.

Some phalanges are preserved in the association (UFSM 11660M), but it is not possible to assign their position in the pes. A non-terminal phalanx was preserved articulated with an ungual (Fig. 14). Their morphology resembles that of other early sauropodomorph phalanges. The non-terminal phalanx is longer than wide and presents a constriction at the mid-length. This condition differs from the stouter phalanx of sauropodiforms. Collateral ligament pits excavate the distal condyles. The ungual phalanx is ventrally curved and presents a conspicuous ridge on the lateral surface. It lacks a well-developed tuber on the ventral surface of the proximal portion.

RESULTS

Phylogenetic analysis

The analysis employing the data matrix of Norman *et al.* (2022) recovered 96 MPTs of 1109 steps (CI = 0.289; RI = 0.680). As expected, UFSM 11660 was recovered within Sauropodomorpha, in a polytomy with the saturnaliids *S. tupiniquim*, *C. novasi*, and *Nhandumirim waldsangae* (Fig. 15). The IterPCR (Pol and Escapa 2009) method was used in order to detect any floating OTUs. The protocol identified *Saltopus elginensis*, *Manidens condorensis*, *Echiodon drummondii*, and *Dongusuchus efremovi* as the main floating OTUs. The reduced strict consensus tree with these OTUs were pruned a posteriori is better resolved, but the Saturnaliidae polytomy is still found.

In the analysis using the data matrix of Langer *et al.* (2022), UFSM 11660 was recovered within *S. tupiniquim* in both scenarios and the general topology was the same as recovered in the former study (Fig. 16). In the per specimen analysis 35 MPTs of 1554 steps (CI = 0.449, RI = 0.449), with UFSM 11660 nested amid the type-series of *S. tupiniquim*. In the analysis with the combined specimens, UFSM 11660 was recovered as the sister-taxon of *S. tupiniquim* (four MPTs of 1464 steps, CI = 0.476, RI = 0.551).

Morphospace occupancy

The analysis recovered a pattern similar to that described by Langer *et al.* (2022) and Moro *et al.* (2024). PCoA1 corresponded to 21.45% of the total variance, whereas PCoA2 corresponded to 16.71% (Fig. 16C). The morphospaces of the hypodigms of *E. lunensis*, *Bu. schultzi*, and *S. tupiniquim* did (including UFSM 11660) not overlap. Additionally, the PERMANOVA recovered a significant difference ($P < .05$) in the position occupied by each of those hypodigms. The plot showing the specimen's positions can be found in the Supporting information.

Skull length estimate

The skull size of UFSM 11660 is estimated in 104.37 mm according to the linear regression ($p = 4.27 \times 10^{-5}$; $R^2 = 0.9403$).

DISCUSSION

Taxonomic assignation

The analysis of the data matrix of Langer *et al.* (2022) provides support to assign UFSM 11660 as a new specimen of *S. tupiniquim*. Similarly, the PERMANOVA recovered a

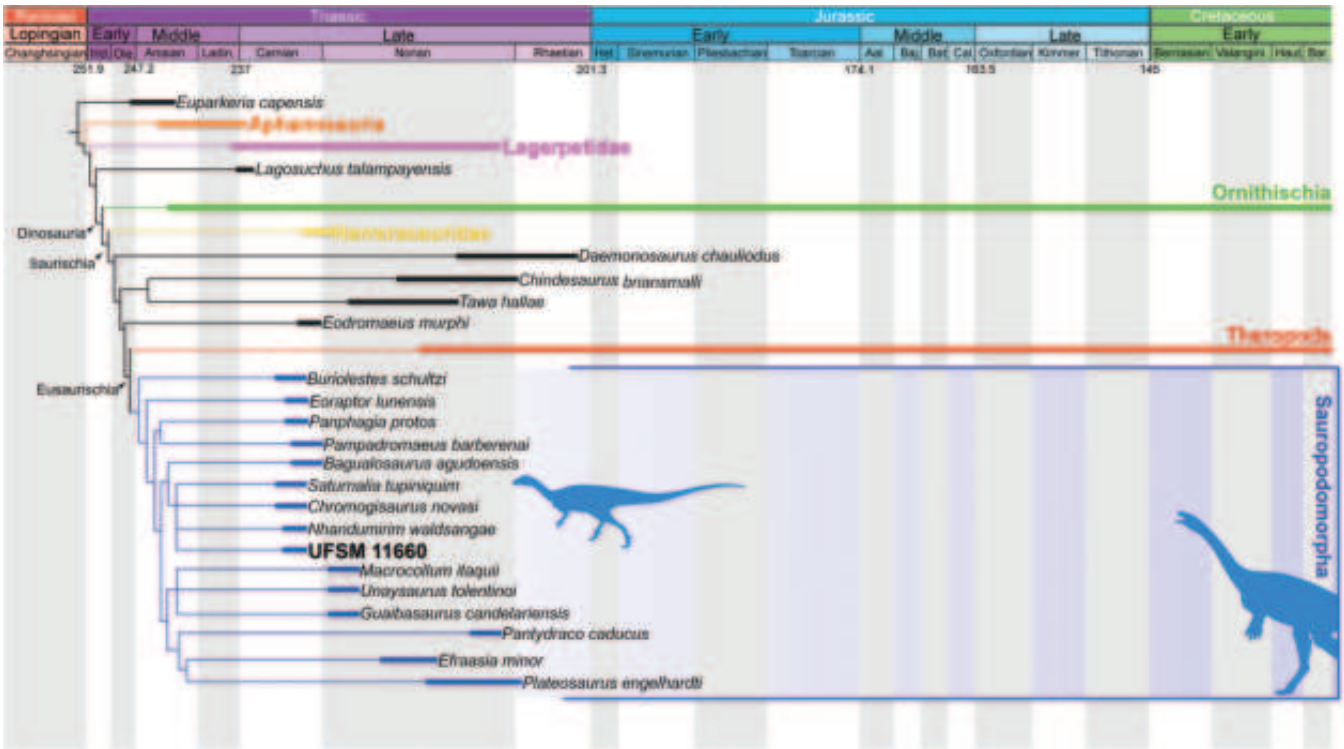

Figure 15. Abbreviated consensus tree of the first phylogenetic analysis.

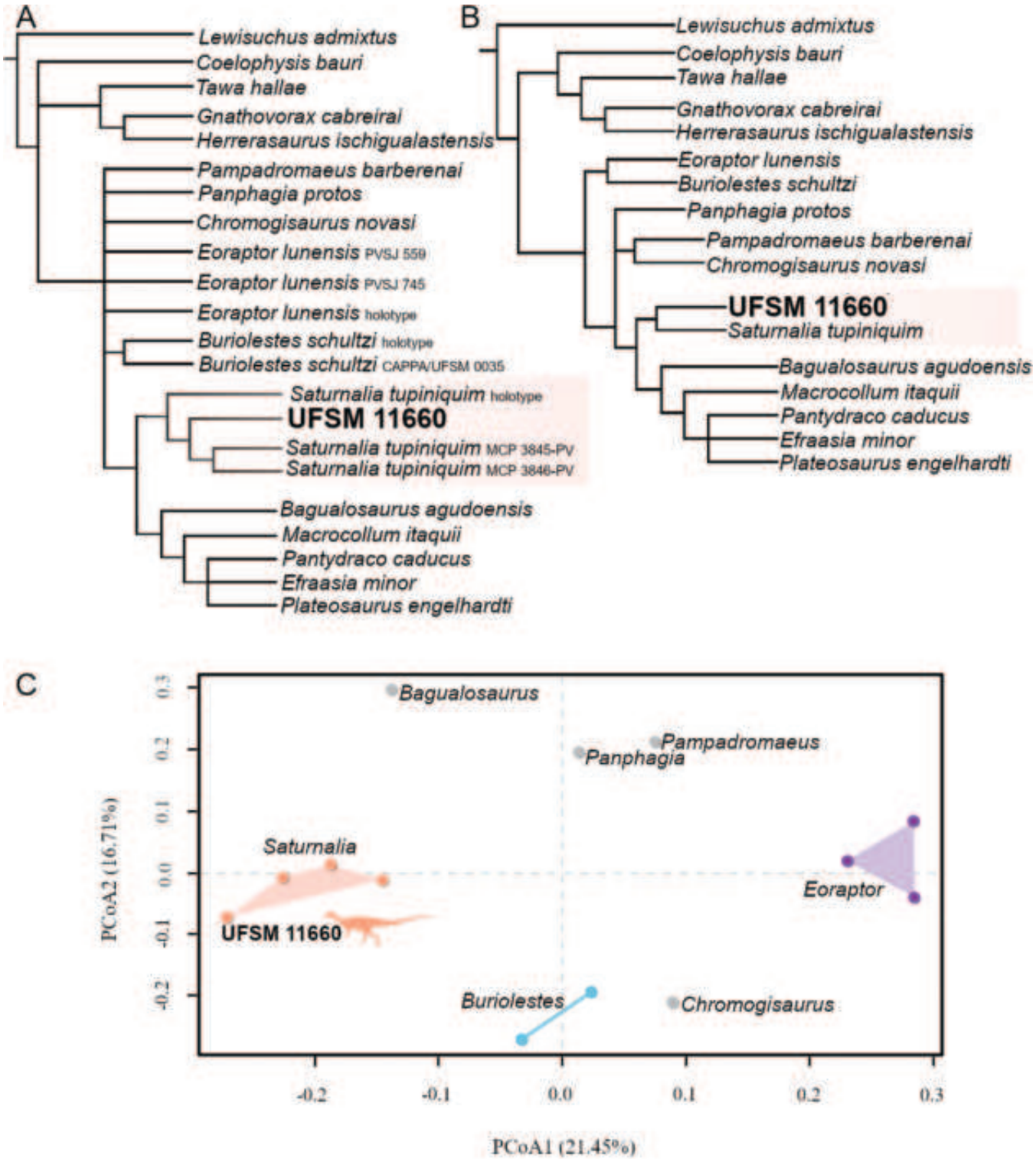

Figure 16. Phylogenetic relations and morphospace position of UFSM 11660 among Carnian sauropodomorphs: (A) per specimen analysis; (B) combined analysis; (C) morphospace represented by PCoA1 (21.45%) and PCoA2 (16.71%). Sauropodomorph silhouette by Maurício S. Garcia.

significant ($p < .05$) difference between the hypodigms of *Bu. schultzi*, *E. lunensis*, and *S. tupiniquim* (including UFSM 11660). Indeed, *S. tupiniquim* differs from other coeval sauropodomorphs based on a unique combination of features (Langer *et al.* 2022), which is observed in the preserved bones of UFSM 11660. In addition, the latter differs from all other coeval sauropodomorphs according to the following list of differences (sources: Table 2; Fig. 17):

Buriolestes schultzi differs from UFSM 11660 in: proportionally longer skull compared to its femoral length; marked gap

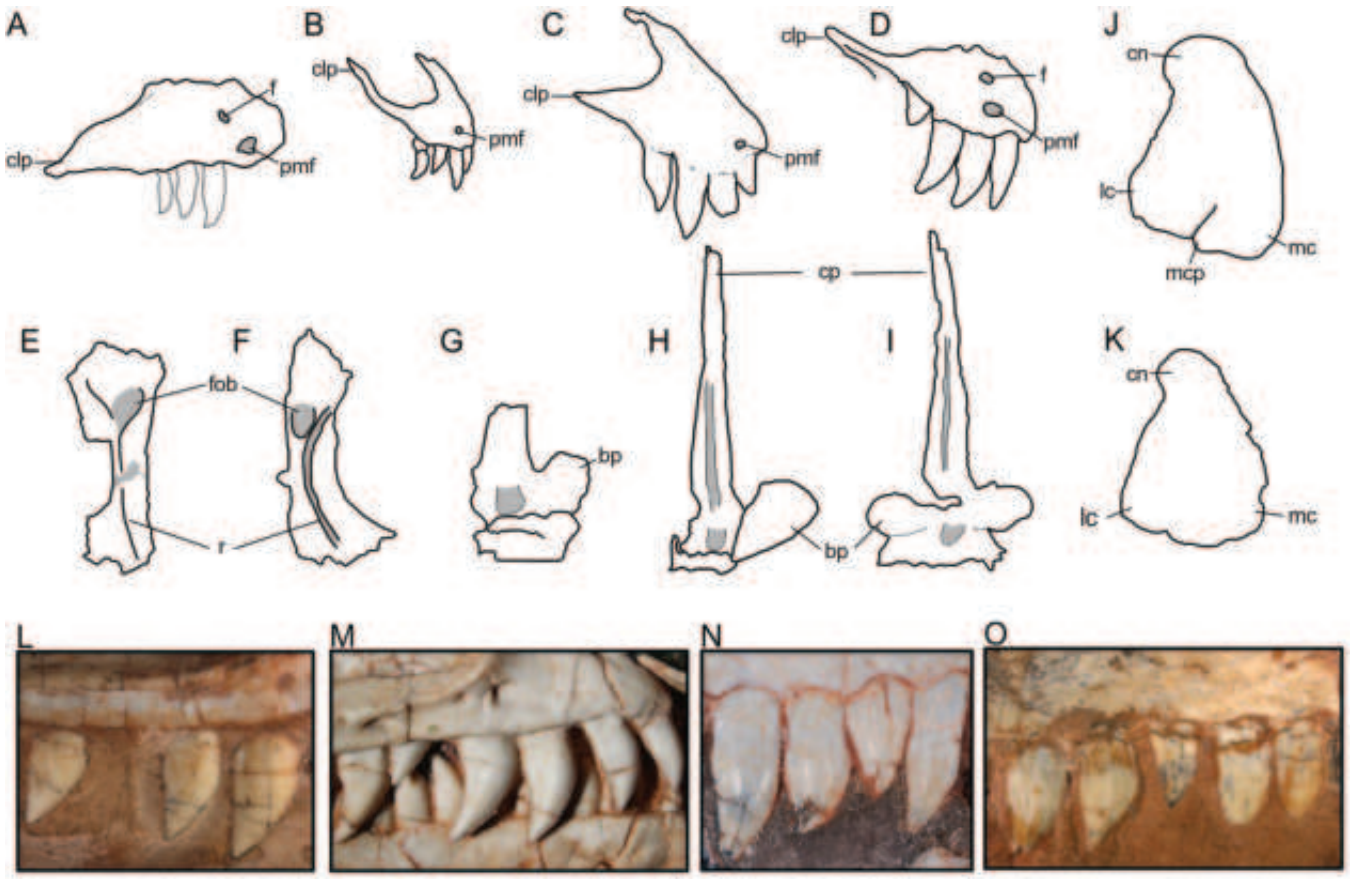

Figure 17. Selected differences among Carnian sauropodomorphs. A–D, Right premaxillae showing the differences in the caudolateral process and number of foramina: (A) UFSM 11660; (B) *Eoraptor lunensis*; (C) *Pampadromaeus barberenai*; (D) *Buriolestes schultzi* (ULBRA-PVT 280). E, F, Left frontal in ventral view of (E) UFSM 11660 composed of one ridge and (F) *Panphagia protos* with two parallel ridges. G–I, Parabasisphenoid in ventral view; it projects anteroventrally in (G) UFSM 11660 and (H) *Saturnalia tupiniquim* (MCP 3845-PV), whereas it projects laterally in (I) *Buriolestes schultzi* (CAPPA/UFSM 0035). J, K, Tibiae in proximal view of (J) UFSM 11660 and *Buriolestes schultzi* (ULBRA-PVT 280). Note that *Bu. schultzi* presents the medial condyle projection. L–O, Anterior maxillary dentition of Carnian sauropodomorphs (L) UFSM 11660*, (M) *Buriolestes schultzi* (ULBRA-PVT 280), (N) *Pampadromaeus barberenai*, (O) *Bagualosaurus agudoensis**. Abbreviations: bp, basipterygoid process; clp, caudolateral process; cn, cnemial crest; cp,cultriform process; f, foramen; fob, fossa for the olfactory bulb; lc, lateral condyle; mc, medial condyle; mcp, medial condyle projection; pmf, premaxillary foramen; r, ridge. Not to scale; * = reversed (redrawn from sources in Table 2).

between the premaxilla and maxilla; excavated area in the rostral region of the maxilla; further maxillary teeth; projection in the lacrimal dorsoventral corner; laterally projected basipterygoid process of the parabasisphenoid; caudal projection of the medial condyle of the tibia.

Chromogisaurus novasi differs from UFSM 11660 in: unexpanded medial condyle of the tibia; markedly asymmetrical distal end of metatarsal II.

Eoraptor lunensis differs from UFSM 11660 in: proportionally longer skull compared to its femoral length; elongated caudoventral process of the premaxilla; no extra foramen above the anterior premaxillary foramen; further maxillary teeth; subtriangular distal end of the ischium.

Panphagia protos differs from UFSM 11660 in: possessing two crests on the ventral margin of the frontal; no postacetabular embayment in the postacetabular ala of the ilium; no conspicuous crest on the lateral surface of the iliac peduncle of the ischium; more laterally arched cnemial crest of the tibia

Pampadromaeus barberenai differs from UFSM 11660 in: proportionally longer skull compared to its femoral length; maxillary teeth serrations forming oblique angles to the main axis of the tooth; no foramen above the anterior premaxillary foramen; further maxillary teeth; intercondylar groove more expanded than the lateral and medial condyles of the femur; hypertrophied fibular condyle of the femur; 'L-shaped' proximal portion of metatarsal I.

Bagualosaurus agudoensis differs from UFSM 11660 in: maxillary teeth serrations forming oblique angles to the main axis of the tooth; no marked fibular crest in the tibia.

Mbiresaurus raathi differs from UFSM 11660 in: ventrally projected ventral margin of the rostral end of the dentary; co-ossified sacral centra (NHMZ 2547); craniodorsally short postacetabular ala of the ilium.

UFSM 11660 was excavated from the type-locality of *S. tupiniquim* and the shared morphology and phylogenetic affinities with its type-material support assigning the new specimen to the species. However, it shares no unequivocal autapomorphies of *S. tupiniquim* and bears some differences when compared to the other specimens. This morphological variation is discussed below in order to highlight putative intraspecific variations for *S. tupiniquim*.

Intraspecific variation in *Saturnalia tupiniquim*

The alpha taxonomy of the earliest sauropodomorphs became a challenging topic after the discovery of several new species and specimens (Müller and Garcia 2020, Langer *et al.* 2022). Because the limits of the intraspecific variation present in these dinosaurs are poorly known, it is important to search for new data on the issue. During the description of UFSM 11660, we observed traits that vary among specimens of *S. tupiniquim*, especially in the pelvic girdle and hindlimb. This is in line with recent works that revealed some degree of variation in the early sauropodomorph *Bu. schultzi* (Müller *et al.* 2018a, Müller 2022, Moro *et al.* 2024).

The ilium of UFSM 11660 presents a muscle scar in the postacetabular ala. As observed by Garcia *et al.* (2019b), among the paratypes of *S. tupiniquim*, MCP 3845-PV has some rugosities in the area, whereas MCP 3846-PV has faint muscle scars. In the holotype (MCP 3844-PV) there is a strongly marked rugosity

Figure 18. Intraspecific variation regarding the hindlimb elements of *S. tupiniquim* and *N. waldsangae*. Femora in (A, D, H, L, P) lateral, (B, E, I, M, Q) cranial, and (C, F, J, N, R) medial views. Tibia in proximal view (G, H, K, O, S). Arrows indicate characters that vary among specimens. Scale bars A-F, H-J, L-N, P-R 50 mm; G, K, O, S 10mm.

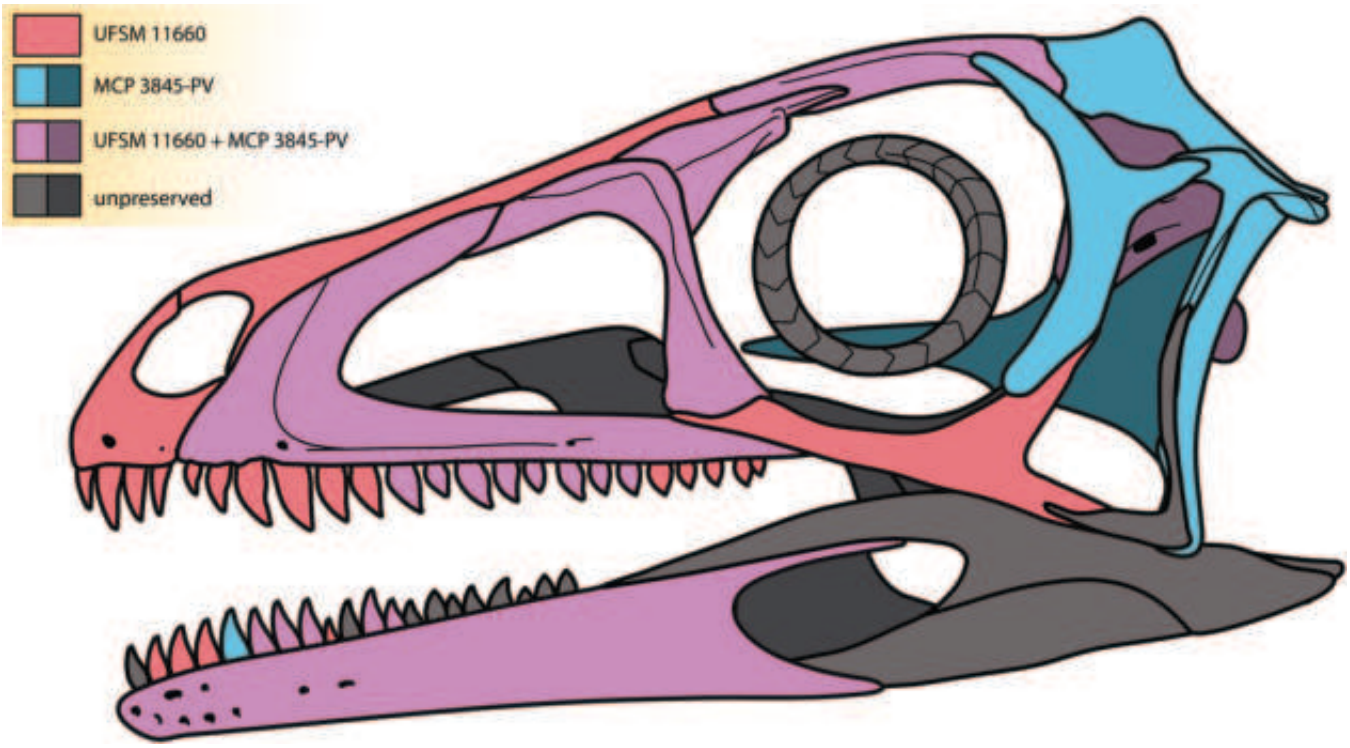

Figure 19. Reconstruction of the skull of *S. tupiniquim* in left lateral view based on the available specimens. Artwork by Maurício Garcia.

in the same area, identified by Langer (2003) as the origin of the muscles the flexor tibialis externus and the iliotibialis. The morphology of the holotype matches the advanced ontogenetic stage proposed by Garcia *et al.* (2019b).

The distal end of the ischial shaft of UFSM 11660 is slightly dorsally expanded, a condition that resembles that of the specimen MCP 3845-PV. On the other hand, the homologous region is more expanded in the holotype of *S. tupiniquim*. The condition observed in the holotype differs from that of other early sauropodomorph (e.g. *Pan. protos*; *Bu. schultzi*) ischia, the distal ends of which are far less expanded.

Considering the femoral anatomy (Fig. 18), the craniolateral scar (sensu Griffin and Nesbitt 2016a) is present in some femora of *S. tupiniquim*. In the type-series, it is well developed only in the left femur of MCP 3845-PV, whereas it seems absent in the right one. Likewise, the scar is well marked in UFSM 11660I, but not in 11660J. This reinforces that the craniolateral scar is a plastic structure (Griffin and Nesbitt 2016a, Müller 2022). Another variable feature in the femora of *S. tupiniquim* is the presence of a faint cleft between the proximal tip of the cranial (= lesser) trochanter and the femoral shaft (Müller *et al.* 2016). Yet, this is seen only in the holotype (MCP 3844-PV), whereas the proximal tip of the cranial trochanter is completely connected to the shaft in the paratypes (MCP 3845-PV; 3846-PV) and UFSM 11660J. Finally, there is also variation regarding the angle formed between the distal margin of the fourth trochanter and the femoral shaft within the type-series (Fig. 18).

We also compared the femoral anatomy of the *S. tupiniquim* hypodigm with that of *Nhandumirim waldsangae*, a juvenile early saurischian sharing the same type-locality (Marsola *et al.* 2019, Pacheco *et al.* 2019). The femur of *N. waldsangae* lacks the trochanteric shelf, a feature that is ontogenetically variable in early dinosauromorphs (Griffin *et al.* 2019). The dorsolateral trochanter is slightly more distally located then in individuals of *S. tupinquim*, which are all more ontogenetically advanced. In fact, the femur of *N. waldsangae* bears juvenile traits recognized in specimens of *Asilisaurus kongwe* (Griffin and Nesbitt 2016a), such as the fourth trochanter formed of a sharp ridge, the presence of a poorly developed cranial (=lesser) trochanter, and the absence of a craniolateral scar. Considering the changes in femoral morphology during ontogeny (Griffin and Nesbitt 2016a, b), it is plausible that the femoral anatomy of a skeletally mature individual of *N. waldsangae* would resemble that of *S. tupiniquim*.

As for the tibia, the *S. tupiniquim* holotype (MCP 3844-PV) has a deep cleft between the medial and lateral condyles, forming a concave area (Fig. 18), whereas the cleft is faint in MCP 3845 and UFSM 11660K. Likewise, although the proximal end of the tibia of MCP 3846 is stouter, the cleft forms only a small incision. In addition, the cnemial crest of MCP 38440-PV is strongly arched laterally, but far less so in UFSM 11660K.

Although some of these differences are subtle, most of them correspond to distinct character states in phylogenetic data matrices (e.g. raised scars on the iliac blade; shape of the proximal tip of the cranial trochanter). A recent study by Müller *et al.* (2024) demonstrated that skeletally immature individuals of early dinosaurs nest together in the phylogenetic trees in response to shared ontogenetic traits. Several authors agree that early dinosaurs had high morphological plasticity during its development (Griffin and Nesbitt 2016a, Müller 2022, Otero and Pol 2022). Therefore, new specimens and additional efforts to clarify the range of the intraspecific variation of early dinosaurs are necessary.

Table 4. Measurements for the ratio of skull and femoral length

Taxa	Skull length (mm)	Femoral length (mm)	Ratio (skull/femur)	Source
Buriolestes schultzi (CAPPA/UFSM 0035)	108.5	136	0.79	Müller *et al.* 2018a
Macrocollum itaquii (CAPPA/UFSM 001a)	147	270	0.54	Müller *et al.* 2020, Personal observation
Macrocollum itaquii (CAPPA/UFSM 001b)	154	364	0.42	Müller *et al.* 2020, Personal observation
Bagualosaurus agudoensis (UFRGS-PV-1099-T)	125.4	225.79	0.55	Pretto *et al.* 2019
Eoraptor lunensis (PVSJ 512)	123	152	0.80	Sereno *et al.* 2013
Plateosaurus trossingensis (SMNS 13200)	321	680	0.47	Galton 1985, Schaeffer 2024
Saturnalia tupiniquim (MCP 3845-PV)	89,5	156	0.57	Bronzati *et al.* 2019b, Langer 2003
Saturnalia tupiniquim (UFSM 11660)	104.37[a]	157	0.66	This contribution
Pampadromaeus barberenai (ULBRA-PVT 016)	124.54[a]	128.16[b]	0.97	Personal observation

[a]Estimated.[b]Note that the femora of *Pampadromaeus* might be affected by sedimentary compression, biasing its measurements.

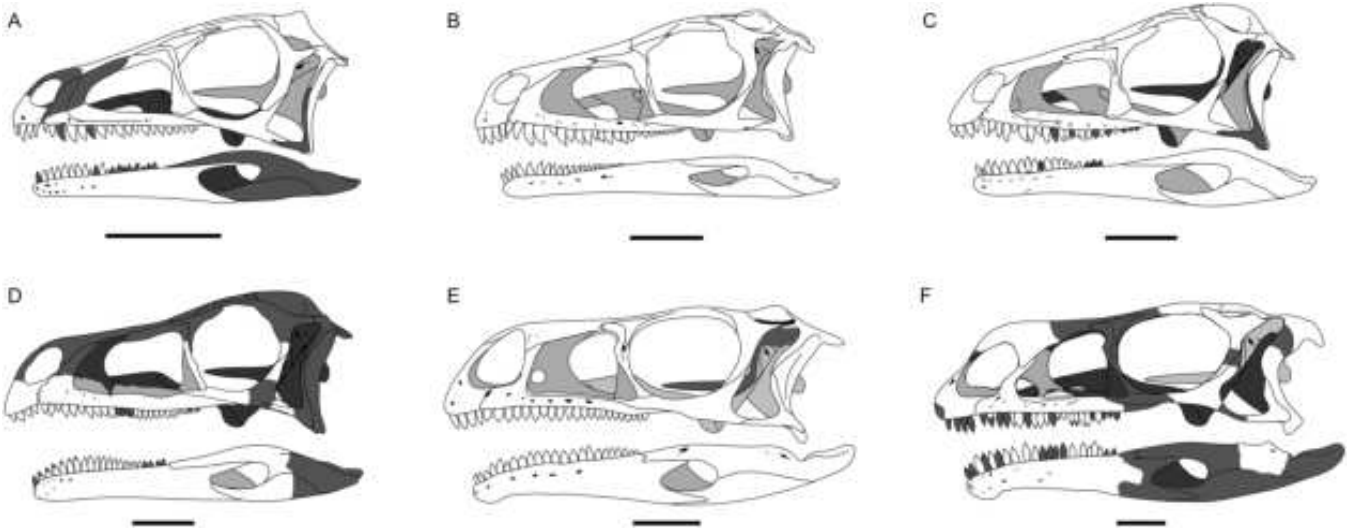

Figure 20. Skulls of some Carnian and Norian sauropodomorphs: (A) *Saturnalia tupiniquim* (based on MCP 3845-PV and UFSM 11660); (B) *Buriolestes schultzi* (based on CAPPA/UFSM 0035), (C) *Pampadromaeus barberenai*, (D) *Bagualosaurus agudoensis*, (E) *Macrocollum itaquii*, (F) *Unaysaurus tolentinoi*. Grey areas = unpreserved bones. Scale = 25 mm. Reconstructions by Maurício S. Garcia.

Rostral anatomy of *Saturnalia tupiniquim*

Although *S. tupiniquim* is one of the best studied Carnian sauropodomorphs (Langer *et al.* 1999, 2007, Langer 2003, Bronzati *et al.* 2017, 2019a, b), its rostral anatomy was unknown until the discovery of UFSM 11660 (Fig. 19), which revealed several phylogenetically significant traits. The premaxilla differs from that of *E. lunensis*, which bears an elongated caudolateral process (Sereno *et al.* 2013). As suggested by Bronzati *et al.* (2017, 2019b), the dentition of *S. tupiniquim* resembles that of *Bu. schultzi*, being composed of ziphodont teeth with small serrations (Cabreira *et al.* 2016, Müller *et al.* 2018a). Conversely, it was initially described as composed of lanceolate and coarsely serrated in the first general description of the taxon (Langer *et al.* 1999). In addition, the maxilla bears 19 tooth positions, contrasting with the 24 positions of *Buriolestes. schultzi* (Müller *et al.* 2018a). The reduced number of tooth positions of UFSM 11660 reflects the proportionally shorter rostrum of *S. tupiniquim*, compared to that of *Bu. schultzi* (CAPPA/UFSM 0035), which matches the difference in relative length between the skulls of both species (see below; Table 4).

The new data on UFSM 11660 provides further support (Bronzati *et al.* 2019b) for a proportionally shorter skull in *S. tupiniquim*, when compared to forms such as *Bur. schultzi* and *E. lunensis* (Sereno *et al.* 2013, Cabreira *et al.* 2016, Müller *et al.* 2018a). This information is particularly interesting because the skull shortening is a typical sauropodomorph trait (Fig. 20; Yates 2007, Langer *et al.* 2009, Bronzati *et al.* 2019b). *Saturnalia tupiniquim* is the oldest sauropodomorph exhibiting this condition, indicating that it was acquired during the early evolutionary history of the group (Fig. 21). Moreover, the rostral anatomy of the new specimen demonstrates that the first steps towards the reduction of the skull occurred by the shortening of the rostrum, as the caudal portion of the skull of *S. tupiniquim* is about the same size as that of taxa with longer skulls (e.g. *Bu. schultzi* and *E. lunensis*). Although remains of *S. tupiniquim* and *Bu. schultzi* have not been excavated from the same site so far, both species are putatively coeval (Müller and Garcia 2020, Novas *et al.* 2021, Langer *et al.* 2022). If this hypothesis is correct, the co-occurrence of two faunivorous sauropodomorphs with distinct skull proportions could demonstrate some degree of niche partitioning.

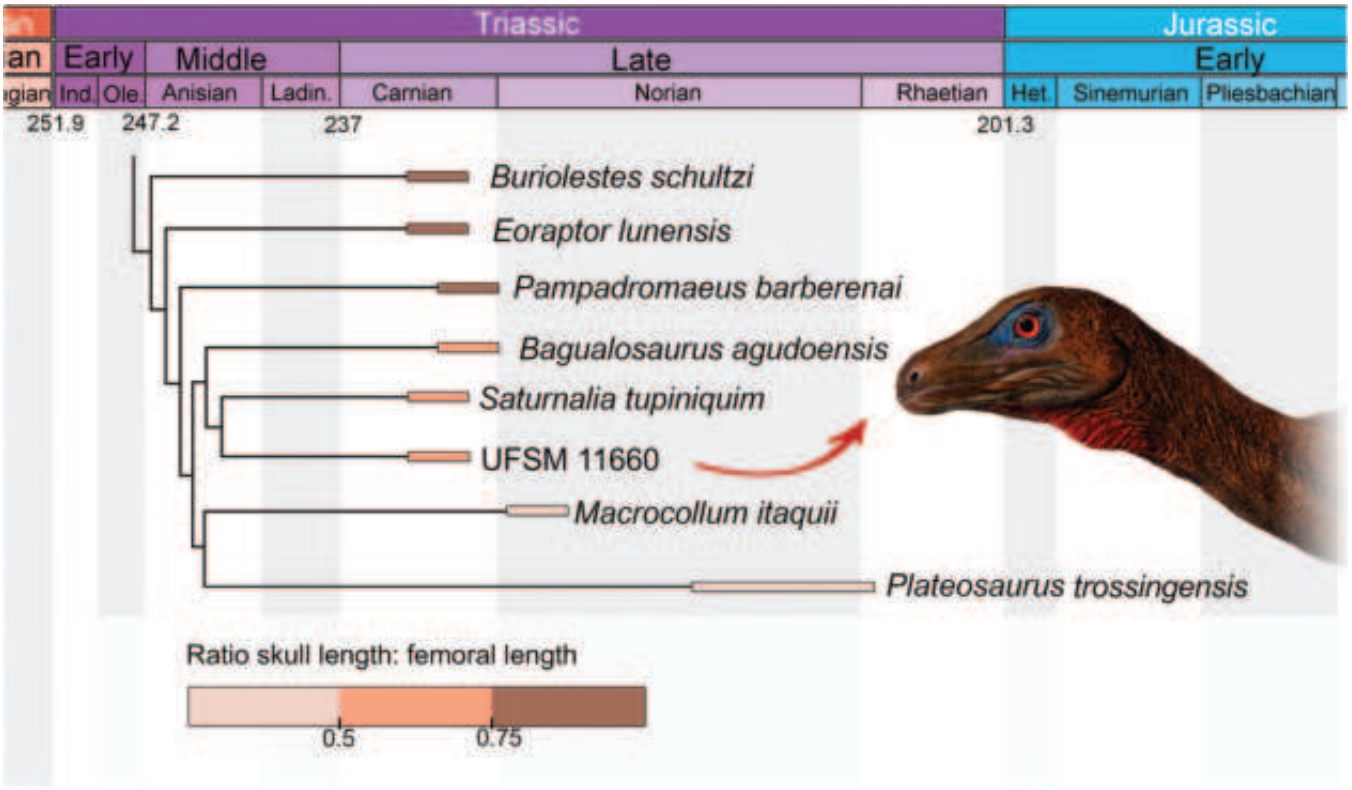

Figure 21. Ratios between skull and femoral length of earliest sauropodomorphs. Life reconstruction of *S. tupiniquim* by Johnny 'Mingau' Pauly Vieira.

CONCLUSION

After 25 years of the first description of the type-series of *Saturnalia tupiniquim*, a new specimen is formally assigned to the species. This attribution is supported by first-hand comparisons, phylogenetic data, and morphospace occupation analyses. The new specimen provides the first record of the rostral anatomy of *S. tupiniquim*, revealing a short rostrum in comparison to that of coeval sauropodomorphs. Although the role of this feature is still uncertain, it was kept in the sauropodomorph lineage, becoming even more marked in post-Carnian forms. The new specimen also revealed variable traits for *S. tupiniquim*, highlighting the need to better understand the limits of the intraspecific variation experienced by the earliest sauropodomorphs, in order to explore the alpha diversity of these animals. Finally, the specimen confirms the presence of a small carnivorous dinosaur in the palaeofauna of the Cerro da Alemoa site, putatively coexisting with large herrerasaurids, silesaurids, and rhynchosaurs (Garcia *et al.* 2021, Mestriner *et al.* 2023).

SUPPORTING INFORMATION

Supplementary data is available at *Zoological Journal of the Linnean Society* online.

ACKNOWLEDGEMENTS

We thank the anonymous reviewers for valuable comments that improved the quality of the manuscript. We also thank the Willi Hennig Society for the gratuity of the TNT software. We acknowledge Voltaire Paes Neto for his contribution on early versions of the manuscript; Maurício Garcia for providing some silhouettes and Figures 19 and 20; and Claire Peyere de Fabrègues for sharing some sauropodomorphs measurements. This work was carried out with aid of Coordenação de Aperfeiçoamento de Pessoal de Nível Superior (CAPES 88887.823241/2023-00) to L.V.S.D.; Fundação de Amparo à Pesquisa do Estado de São Paulo (20/07997-4) to M.C.L.; Conselho Nacional de Desenvolvimento Científico e Tecnológico (CNPq 303972/2021-1) to Á.A.S.D.R.; and Conselho Nacional de Desenvolvimento Científico e Tecnológico (CNPq 404095/2021-6; 303034/2022-0; and 406902/2022-4) to R.T.M.

CONFLICT OF INTEREST

The authors declare no competing interests.

REFERENCES

Andreis RR, Bossi GE, Montardo DK. *O Grupo Rosário do Sul (Triássico) no Rio Grande do Sul. Congresso Brasileiro de Geologia* 1980;**31**:659–73.

Apaldetti C, Martinez RN, Alcober OA *et al.* A new basal sauropodomorph (Dinosauria: Saurischia) from Quebrada del Barro Formation (Marayes-El Carrizal Basin), northwestern Argentina. *PLoS One* 2011;**6**:e26964. https://doi.org/10.1371/journal.pone.0026964

Apaldetti C, Pol D, Ezcurra MD *et al.* Sauropodomorph evolution across the Triassic–Jurassic boundary: body size, locomotion, and their influence on morphological disparity. *Scientific Reports* 2021;**11**:22534. https://doi.org/10.1038/s41598-021-01120-w

Baron MG, Norman DB, Barrett PM. A new hypothesis of dinosaur relationships and early dinosaur evolution. *Nature* 2017;**543**:501–6. https://doi.org/10.1038/nature21700

Bittencourt JS, Kellner AWA. The anatomy and phylogenetic position of the Triassic dinosaur *Staurikosaurus pricei* Colbert, 1970. *Zootaxa* 2009;**2079**:1–56.

Bittencourt JS, Leal LA, Langer MC *et al.* An additional basal sauropodomorph specimen from the Upper Triassic Caturrita Formation, southern Brazil, with comments on the biogeography of plateosaurids. *Alcheringa: An Australasian Journal of Palaeontology* 2012;**36**:269–78. https://doi.org/10.1080/03115518.2012.634111

Brochu CA. Closure of neurocentral sutures during crocodilian ontogeny: implications for maturity assessment in fossil archosaurs. *Journal of Vertebrate Paleontology* 1996;**16**:49–62. https://doi.org/10.1080/02724634.1996.10011283

Bronzati M, Rauhut OWM, Bittencourt JS *et al.* Endocast of the Late Triassic (Carnian) dinosaur *Saturnalia tupiniquim*: implications for the evolution of brain tissue in Sauropodomorpha. *Scientific Reports* 2017;**7**:11931. https://doi.org/10.1038/s41598-017-11737-5

Bronzati M, Langer MC, Rauhut OWM. Braincase anatomy of the early sauropodomorph *Saturnalia tupiniquim* (Late Triassic, Brazil). *Journal of Vertebrate Paleontology* 2019a;**38**:e1559173.

Bronzati M, Müller RT, Langer MC. Skull remains of the dinosaur *Saturnalia tupiniquim* (Late Triassic, Brazil): with comments on the early evolution of sauropodomorph feeding behaviour. *PLoS One* 2019b;**14**:e0221387. https://doi.org/10.1371/journal.pone.0221387

Cabreira SF, Schultz CL, Bittencourt JS *et al.* New stem-sauropodomorph (Dinosauria, Saurischia) from the Triassic of Brazil. *Naturwissenschaften* 2011;**98**:1035–40. https://doi.org/10.1007/s00114-011-0858-0

Cabreira SF, Kellner AWA, Dias da Silva S *et al.* A unique Late Triassic Dinosauromorph assemblage reveals dinosaur ancestral anatomy and diet. *Current Biology* 2016;**26**:3090–5.

Carabajal AP. Neuroanatomy of titanosaurid dinosaurs from the Upper Cretaceous of Patagonia, with comments on endocranial variability within Sauropoda. *Anatomical Record* 2012;**295**:2141–56. https://doi.org/10.1002/ar.22572

Da-Rosa AAS. Geological context of the dinosauriform-bearing outcrops from the Triassic of Southern Brazil. *Journal of South American Earth Sciences* 2015;**61**:108–19.

Dunne EM, Farnsworth A, Benson RBJ *et al.* Climatic controls on the ecological ascendancy of dinosaurs. *Current Biology* 2023;**33**:206–14.e4. https://doi.org/10.1016/j.cub.2022.11.064

Ezcurra MD. A new early dinosaur (Saurischia: Sauropodomorpha) from the Late Triassic of Argentina: a reassessment of dinosaur origin and phylogeny. *Journal of Systematic Palaeontology* 2010;**8**:371–425.

Ezcurra MD, Nesbitt SJ, Bronzati M *et al.* Enigmatic dinosaur precursors bridge the gap to the origin of Pterosauria. *Nature* 2020;**588**(7838):445–9.

Fabbri M *et al.* Sauropodomorpha. In: de Queiroz K, Cantino PD, Gauthier JA (eds), *Phylonyms: a Companion to the PhyloCode*, 2020, 1225–34.

Galton PM. ranial anatomy of the prosauropod dinosaurPlateosaurus from the Knollenmergel (Middle Keuper, Upper Triassic)of Germany. II. All the cranial material and details of soft-part anat-omy. *Geologica et Palaeontologica,* 1985;**19**:119–59.

Garcia MS, Müller RT, Da-Rosa AAS *et al.* The oldest known co-occurrence of dinosaurs and their closest relatives: a new lagerpetid from a Carnian (Upper Triassic) bed of Brazil with implications for dinosauromorph biostratigraphy, early diversification and biogeography. *Journal of South American Earth Sciences* 2019a;**91**:302–19.

Garcia MS, Pretto FA, Dias-da-Silva S *et al.* A dinosaur ilium from the Late Triassic of Brazil with comments on key-character supporting Saturnaliinae. *Anais da Academia Brasileira de Ciencias* 2019b;**91**:e20180614. https://doi.org/10.1590/0001-3765201920180614

Garcia MS, Müller RT, Pretto FA *et al.* Taxonomic and phylogenetic reassessment of a large-bodied dinosaur from the earliest dinosaur-bearing beds (Carnian, Upper Triassic) from southern Brazil. *Journal of Systematic Palaeontology* 2021;**19**:1–37.

Gauthier JA, Langer MC, Novas FE *et al.* Saurischia. In: de Queiroz K, Cantino PD, Gauthier JA (eds), *Phylonyms: a Companion to the PhyloCode*, 2020;**1**:1219–24.

Griffin CT, Nesbitt SJ. The femoral ontogeny and long bone histology of the Middle Triassic (? Late Anisian) dinosauriform *Asilisaurus kongwe* and implications for the growth of early dinosaurs. *Journal of Vertebrate Paleontology* 2016a;**36**:e1111224. https://doi.org/10.1080/02724634.2016.1111224

Griffin CT, Nesbitt SJ. Anomalously high variation in postnatal development in ancestral for dinosaurs but lost in birds. *Proceedings of the National Academy of Sciences* 2016b;**113**:14757–62.

Griffin CT, Bano LS, Turner AH *et al.* Integrating gross morphology and bone histology to assess skeletal maturity in early dinosauromorphs: new insights from *Dromomeron* (Archosauria: Dinosauromorpha). *PeerJ* 2019;**7**:e6331. https://doi.org/10.7717/peerj.6331

Griffin CT, Wynd BM, Munyikwa D *et al.* Africa's oldest dinosaurs reveal early suppression of dinosaur distribution. *Nature* 2022;**609**:313–9. https://doi.org/10.1038/s41586-022-05133-x

Heinrich C, Paes-Neto VD, Lacerda MB *et al.* The ontogenetic pattern of neurocentral suture closure in the axial skeleton of Hyperodapedontinae (Archosauromorpha, Rhynchosauria) and its evolutionary implications. *Palaeontology* 2021;**64**:409–27.

Horn BLD, Melo TM, Schultz CL *et al.* A new third-order sequence stratigraphic frame-work applied to the Triassic of the Paraná Basin, Rio Grande do Sul, Brazil, based on structural, stratigraphic and paleontological data. *Journal of South American Earth Sciences* 2014;**55**:123–32. https://doi.org/10.1016/j.jsames.2014.07.007

Huene F. Die fossile Reptil-Ordnung Saurischia, ihre Entwicklung und Geschichte. *Monographien zur Geologie und Paläontologie* 1932;**4**:1–361.

Irmis RB. Axial skeleton ontogeny in the Parasuchia (Archosauria: Pseudosuchia) and its implications for ontogenetic determination in archosaurs. *Journal of Vertebrate Paleontology* 2007;**27**:350–61. https://doi.org/10.1671/0272-4634(2007)27[350:asoitp]2.0.co;2

Langer MC. The pelvic and hind limb anatomy of the stem-sauropodomorph *Saturnalia tupiniquim* (Late Triassic, Brazil). *PaleoBios* 2003;**23**:1–30.

Langer MC. Studies on continental Late Triassic tetrapod biochronology. I. The type locality of *Saturnalia tupiniquim* and the faunal succession in south Brazil. *Journal of South American Earth Sciences* 2005;**19**:205–18. https://doi.org/10.1016/j.jsames.2005.04.003

Langer MC, Abdala F, Richter M *et al.* A sauropodomorph dinosaur from the Upper Triassic (Carman) of southern Brazil. *Comptes Rendus de l'Académie des Sciences - Series IIA - Earth and Planetary Science* 1999;**329**:511–7.https://doi.org/10.1016/s1251-8050(00)80025-7

Langer MC, Ribeiro AM, Schultz CL *et al.* The continental tetrapod-beating Triassic of South Brazil. *New Mexico Museum of Natural History and Science Bulletin* 2007a;**41**:201–18.

Langer MC, França MAG, Gabriel S. The pectoral girdle and forelimb anatomy of the stem-sauropodomorph *Saturnalia tupiniquim* (Upper Triassic, Brazil). *Special Papers in Palaeontology* 2007b;**77**:113–37.

Langer MC, Ezcurra MD, Bittencourt JS *et al.* The origin and early evolution of dinosaurs. *Biological Reviews* 2009;**85**:55–110. https://doi.org/10.1111/j.1469-185X.2009.00094.x

Langer MC, Ezcurra MD, Rauhut O *et al.* Untangling the dinosaur family tree. *Nature* 2017;**551**:E1–3.

Langer MC, Ramezani L, Da Rosa AAS. U-Pb age constraints on dinosaur rise from south Brazil. *Gondwana Research* 2018;**57**:133–40.

Langer MC, McPhee BW, Marsola JC *et al.* Anatomy of the dinosaur *Pampadromaeus barberenai* (Saurischia—Sauropodomorpha) from the Late Triassic Santa Maria Formation of southern Brazil. *PLoS One* 2019;**14**:1–64.

Langer MC, Novas FE, Bittencourt JS *et al.* Dinosauria. In: de Queiroz K, Cantino PD, Gauthier JA (eds), *Phylonyms: a Companion to the PhyloCode*, 2020, 1209–17.

Langer MC, Marsola JCA, Müller R *et al.* The Early Radiation of Sauropodomorphs in the Carnian (Late Triassic) of South America. In: Otero A, Carballido JL, Pol D (eds), *South American Sauropodomorph Dinosaurs: record, diversity and evolution*. Switzerland: Springer, 2022, 1–582.

Leal LA, Azevedo SAK, Kellner AWA *et al.* A new early dinosaur (Sauropodomorpha) from the Caturrita Formation (Late Triassic), Paraná Basin, Brazil. *Zootaxa* 2004;**690**:1–24.

Lehmann OE, Ezcurra MD, Buttler RJ *et al.* Biases with the generalized euclidean distance measure in disparity analyses with high levels of missing data. *Palaeontology* 2019;**62**:837–49.

Lloyd GT. Estimating morphological diversity and tempo with discrete character-taxon matrices: implementation, challenges, progress and future directions. *Biological Journal of the Linnean Society* 2016;**118**:131–51. https://doi.org/10.1111/bij.12746

Marsola JCA, Bittencourt JS, Butler RJ *et al.* A new dinosaur with theropod affinities from the Late Triassic Santa Maria Formation, south Brazil. *Journal of Vertebrate Paleontology* 2019;**38**:e1531878. https://doi.org/10.1080/02724634.2018.1531878

Martinelli AG, Eltink E, Da-Rosa AAS *et al.* New cynodont from the Santa Maria Formation, South Brazil, improves Late Triassic probainognathian diversity. *Papers in Palaeontology* 2017;**3**:401–23.

Martínez RN, Alcober OA. A basal sauropodomorph (Dinosauria: Saurischia) from the Ischigualasto formation (Triassic, Carnian) and the early evolution of Sauropodomorpha. *PLoS One* 2009;**4**:e4397–12. https://doi.org/10.1371/journal.pone.0004397

Martínez RN, Haro JA, Apaldetti C. Braincase of *Panphagia protos* (Dinosauria, Sauropodomorpha). *Journal of Vertebrate Paleontology* 2013;**2013**:70–82.

McPhee BW, Benson RBJ, Botha JB *et al.* A giant dinosaur from the Earliest Jurassic of South Africa and the transition to quadrupedality in early sauropodomorphs. *Current Biology* 2018;**28**:3143–51.e7.

Mestriner G, Marsola JCA, Nesbitt SJ *et al.* Anatomy and phylogenetic affinities of a new silesaurid assemblage from the Carnian beds of south Brazil. *Journal of Vertebrate Paleontology* 2023;**43**:e2232426.

Moro D, Damke LVS, Müller RT *et al.* An unusually robust specimen attributed to *Buriolestes schultzi* (Dinosauria: Sauropodomorpha) from the Late Triassic of southern Brazil. *Anatomical Record* 2024;**307**:1025–59. https://doi.org/10.1002/ar.25319

Müller RT. Craniomandibular osteology of *Macrocollum itaquii* (Dinosauria: Sauropodomorpha) from the Late Triassic of southern Brazil. *Journal of Systematic Palaeontology* 2020;**18**:805–41.

Müller RT. On the presence and shape of anterolateral scars in the ontogenetic series of femora for two early sauropodomorph dinosaurs from the Upper Triassic of Brazil. *Paleontological Research* 2022;**26**:1–7.

Müller RT, Garcia MS. A paraphyletic 'Silesauridae' as an alternative hypothesis for the initial radiation of ornithischian dinosaurs. *Biology Letters* 2020;**16**:20200417. https://doi.org/10.1098/rsbl.2020.0417

Müller RT, Langer MC, Cabreira SF *et al.* The femoral anatomy of *Pampadromaeus barberenai* based on a new specimen from the Upper Triassic of Brazil. *Historical Biology* 2016;**28**:656–65. https://doi.org/10.1080/08912963.2015.1004329

Müller RT, Langer MC, Bronzati M *et al.* Early evolution of sauropodomorphs: anatomy and phylogenetic relationships of a remarkably well-preserved dinosaur from the Upper Triassic of southern Brazil. *Zoological Journal of the Linnean Society* 2018a;**184**:1187–248.

Müller RT, Garcia MS, Da-Rosa AAS *et al.* Under pressure: effect of sedimentary compression on the iliac morphology of early sauropodomorphs. *Journal of South American Earth Sciences* 2018b;**88**:345–51. https://doi.org/10.1016/j.jsames.2018.09.005

Müller RT, Langer MC, Dias-da-Silva S. An exceptionally preserved association of complete dinosaur skeletons reveals the oldest long-necked sauropodomorphs. *Biology Letters* 2018c;**14**:20180633. https://doi.org/10.1098/rsbl.2018.0633

Müller RT, Ferreira JD, Pretto FA *et al.* The endocranial anatomy of *Buriolestes schultzi* (Dinosauria: Saurischia) and the early evolution of brain tissues in sauropodomorph dinosaurs. *Journal of Anatomy* 2020;**238**:809–27.

Müller RT, Damke LVS, Terras R. Skeletally immature individuals nest together in the phylogenetic tree of early dinosaurs. *Anais da Academia Brasileira de Ciências* 2024;**96**:e20231248.

Nesbitt SJ. The early evolution of archosaurs: relationships and the origin of major clades. *Bull. Am. Mus. Nat. Hist.* 2011;**352**:1–292.

Nesbitt SJ, Smith ND, Irmis RB *et al.* A complete skeleton of a Late Triassic saurischian and the early evolution of dinosaurs. *Science* 2009;**326**:1530–3. https://doi.org/10.1126/science.1180350

Norman DB, Baron MG, Garcia MS *et al.* Taxonomic, palaeobiological and evolutionary implications of a phylogenetic hypothesis for Ornithischia (Archosauria: Dinosauria). *Zoological Journal of the Linnean Society* 2022;**196**:1273–309. https://doi.org/10.1093/zoolinnean/zlac062

Novas FE. New information on the systematics and postcranial skeleton of *Herrerasaurus ischigualastensis* (Theropoda: Herrerasauridae) from the Ischigualasto Formation (Upper Triassic) of Argentina. *Journal of Vertebrate Paleontology* 1994;**13**:400–23. https://doi.org/10.1080/02724634.1994.10011523

Novas FE, Agnolin FL, Ezcurra MD *et al.* Review of the fossil record of early dinosaurs from South America, and its phylogenetic implications. *Journal of South American Earth Sciences* 2021;**110**:103341. https://doi.org/10.1016/j.jsames.2021.103341

Otero A, Pol D. Ontogenetic changes in the postcranial skeleton of Mussaurus patagonicus (Dinosauria, Sauropodomorpha) and their impact on the phylogenetic relationships of early sauropodomorphs. *Journal of Systematic Palaeontology* 2022;**19**:1467–516. https://doi.org/10.1080/14772019.2022.2039311

Owen R. Report on British fossil reptiles. Part II. *Reports of the British Association for the Advancement of Science* 1842;**11**:60–204.

Pacheco C, Müller RT, Langer MC *et al. Gnathovorax cabreirai*: a new early dinosaur and the origin and initial radiation of predatory dinosaurs. *PeerJ* 2019;**7**:e7963. https://doi.org/10.7717/peerj.7963

Piechowski R, Talanda M, Dzik J. Skeletal variation and ontogeny of the Late Triassic dinosauriform *Silesaurus opolensis*. *Journal of Vertebrate Paleontology* 2014;**34**:1383–93. https://doi.org/10.1080/02724634.2014.873045

Pol D, Escapa H. Unstable taxa in cladistic analysis: identification and the assessment of relevant characters. *Cladistics* 2009;**25**:515–27.

Pretto FA, Langer MC, Schultz CL. A new dinosaur (Saurischia: Sauropodomorpha) from the Late Triassic of Brazil provides insights on the evolution of sauropodomorph body plan. *Zoological Journal of the Linnean Society* 2018;**185**:388–416. https://doi.org/10.1093/zoolinnean/zly028

Prieto-Márquez A, Norell MA. Redescription of a nearly complete skull of *Plateosaurus* (Dinosauria: Sauropodomorpha) from the Late Triassic of Trossingen (Germany). *American Museum Novitates* 2011;**3727**:1–58. https://doi.org/10.1206/3727.2

Schaeffer J. Osteological redescription of the holotype of *Plateosaurus trossingensis* (Dinosauria: Sauropodomorpha) from the Upper Triassic of SW Germany and its phylogenetic implications. *Journal of Systematic Palaeontology* 2024;**22**:2335387.

Schultz CL, Martinelli AG, Soares MB *et al.* Triassic faunal successions of the Paraná Basin, southern Brazil. *Journal of South American Earth Sciences* 2020;**104**:102846. https://doi.org/10.1016/j.jsames.2020.102846

Seeley HG. On the classification of the fossil animals commonly named Dinosauria. *Proceedings of the Royal Society of London* 1888;**43**:165–71.

Sereno PC, Novas FE. The skull and neck of the basal theropod *Herrerasaurus ischigualastensis*. *Journal of Vertebrate Paleontology* 1993;**13**:451–76.

Sereno PC, Martínez RN, Alcober OA. Osteology of *Eoraptor lunensis* (Dinosauria, Sauropodomorpha). *Journal of Vertebrate Paleontology* 2013;**32**:83–179.

Yates AM. The first complete skull of the Triassic dinosaur *Melanorosaurus* Haughton (Sauropodomorpha: Anchisauria). *Special Papers in Palaeontology* 2007;**77**:9–55.

Zerfass H, Lavina EL, Schultz CL *et al.* Sequence stratigraphy of continental Triassic strata of southernmost Brazil: a contribution to southwestern Gondwana palaeogeography and palaeoclimate. *Sedimentary Geology* 2003;**161**:85–105. https://doi.org/10.1016/s0037-0738(02)00397-4